THE JOURNAL OF BIOLOGICAL CHEMISTRY VOL. 287, NO. 28, pp. 24026–24042, July 6, 2012

Signaling Active CD95 Receptor Molecules Trigger Co-translocation of Inactive CD95 Molecules into Lipid Rafts*[S]

Received for publication, November 28, 2011, and in revised form, May 4, 2012 Published, JBC Papers in Press, May 29, 2012, DOI 10.1074/jbc.M111.328211

Isabell Lang[‡], Andrea Fick[‡], Viktoria Schäfer[‡], Tina Giner[§], Daniela Siegmund[‡], and Harald Wajant[‡1]

From the [‡]Division of Molecular Internal Medicine, Department of Internal Medicine II, University Hospital Würzburg, Röntgenring 11, 97070 Würzburg, Germany and the [§]Department of Dermatology, University Hospital Würzburg, Josef-Schneider-Str. 2, 97080 Würzburg, Germany

Background: Mechanisms of activation of the prototypical death receptor CD95 have been described.
Results: Highly active CD95L variants (Fc-CD95L, membrane CD95L) stimulate the association of unliganded CD40-CD95 chimeras or of inactive complexes of CD95L trimers and CD95 with the lipid raft compartment.
Conclusion: CD95 signaling triggers association of active and inactive CD95 species with lipid rafts.
Significance: Identification of inactive CD95 species as targets of their active counterparts is described.

The capability of soluble CD95L trimers to trigger CD95-associated signaling pathways is drastically increased by oligomerization. The latter can be achieved, for example, by antibodies recognizing a N-terminal epitope tag in recombinant CD95L variants or by genetic engineering-enforced formation of hexamers. Using highly sensitive and accurate binding studies with recombinant CD95L variants equipped with a *Gaussia princeps* luciferase reporter domain, we found that oligomerization of CD95L has no major effect on CD95 occupancy. This indicates that the higher activity of oligomerized CD95L trimers is not related to an avidity-related increase in apparent affinity and points instead to a crucial role of aggregation of initially formed trimeric CD95L-CD95 complexes in CD95 activation. Furthermore, binding of soluble CD95L trimers was found to be insufficient to increase the association of CD95 with the lipid raft-containing membrane fraction. However, when *Gaussia princeps* luciferase-CD95L trimers were used as tracers to "mark" inactive CD95 molecules, increased association of these inactive receptors was observed upon activation of the remaining CD95 molecules by help of highly active hexameric Fc-CD95L or membrane CD95L. Moreover, in cells expressing endogenous CD95 and chimeric CD40-CD95 receptors, triggering of CD95 signaling via endogenous CD95 resulted in co-translocation of CD40-CD95 to the lipid raft fraction, whereas vice versa activation of CD95-associated pathways with Fc-CD40L via CD40-CD95 resulted in co-translocation of endogenous CD95. In sum, this shows that signaling-active CD95 molecules not only enhance their own association with the lipid raft-containing membrane fraction but also those of inactive CD95 molecules.

CD95 (apo-1, Fas) is the prototypic representative of the death receptor subgroup of the tumor necrosis factor (TNF) receptor family. The extracellular part of CD95 possesses three cysteine-rich domains determining the affiliation to the TNF receptor family. The intracellular part of the molecule further contains a conserved protein-protein interaction domain, called the death domain (DD),[2] that assigns the molecule to the death receptor subgroup and allows activation of the extrinsic pathway of apoptosis (1). The latter relies on the sequential recruitment of the adapter protein Fas-associated death domain (FADD) and the FADD-interacting initiator caspase procaspase-8 to activated CD95. FADD is a bipartite protein comprising C-terminally a DD and N-terminally a death effector domain, a protein-protein interaction domain structurally related to the DD. Thus, FADD links CD95 and procaspase-8 by undergoing homotypic protein-protein interactions with the DD of CD95 and the two death effector domains contained in the prodomain of procaspase-8 (2, 3). CD95 also recruits the DD-containing serine/threonine kinase receptor interacting protein-1. With the help of FADD and receptor interacting protein-1, CD95 is able to trigger a second, caspase-independent mode of cell death, called necrosis (4). CD95 also stimulates non-cytotoxic signaling pathways leading to activation of MAP kinases, the PI3K/Akt pathway, or transcription factors of the NFκB family (2, 3). Activation of the classical NFκB pathway by CD95 requires FADD, receptor interacting protein-1, and caspase-8, whereby the enzymatic activity of the latter seems to be dispensable (5).

CD95-associated signaling pathways can be triggered naturally by CD95L but also by the help of agonistic antibodies. CD95L, like other members of the TNF ligand family, is initially expressed as a type II transmembrane protein and consists of an N-terminal cytoplasmic domain, a single transmembrane helix, a stalk region, and a C-terminal TNF homology domain (THD), the characteristic structural feature of the TNF ligand family (6). The THD drives assembly into homotrimeric molecules and mediates CD95 binding. Metalloproteinases are able to

* This work was supported by Deutsche Forschungsgemeinschaft Grants DFG Wa 1025/21-1 and SFB 487, TP B7.
[S] This article contains supplemental Fig. 1.
[1] To whom correspondence should be addressed. Tel.: 49-931-201-71010; Fax: 49-931-201-71070; E-mail: harald.wajant@mail.uni-wuerzburg.de.

[2] The abbreviations used are: DD, death domain; CHX, cycloheximide; FADD, Fas-associated death domain; FAP, fibroblast activation protein; FLIP, FLICE inhibitory protein; GpL, *G. princeps* luciferase; IκB, inhibitor of κB; MIL, *M. longa* luciferase; NFκB, nuclear factor κB; SEAP, secreted alkaline phosphatase; TNC, tenascin-C; zVAD-fmk, benzyloxycarbonyl-Val-Ala-Asp (OMe) fluoromethyl ketone; THD, TNF homology domain.

process CD95L in the stalk region under release of soluble CD95L trimers (7–10). Soluble CD95L still contains the THD and consequently retains the capability to interact with CD95. Noteworthy, soluble CD95L trimers are poorly active and can even exert an inhibitory effect on membrane CD95L-induced CD95 signaling (8–10).

It has been shown that the impaired/limited response of CD95 toward soluble CD95L can be overcome artificially in two ways; first, by dimerization or oligomerization of soluble CD95L trimers. This can be achieved using epitope-tagged recombinant soluble CD95L and tag-specific antibodies or by fusion of soluble CD95L with a second dimerizing protein domain by genetic engineering (7). Second, impaired/limited response may be overcome by conjunction of soluble CD95L to the cell surface or the extracellular matrix, *e.g.* by use of antibody fusion proteins of soluble CD95L recognizing a cell surface-expressed antigen (11–13). Worth mentioning, both of these possibilities could reflect physiologically relevant situations. In the bronchoalveolar lavage fluid derived from patients with lung injury, highly active aggregates of soluble CD95L are formed secondarily by oxidation (14), and binding of soluble CD95L to fibronectin potentiates its cytotoxic activity (15). Thus, the formation of CD95 signaling complexes and activation of intracellular signaling pathways are not a simple straightforward result of CD95L binding. Indeed, a considerable number of studies show in sum that robust activation of CD95-associated signaling pathways in response to binding of CD95L or agonistic antibodies involves several distinct events (16, 17). Particularly, there is evidence that formation of supramolecular CD95 clusters has a pivotal role in CD95 signaling. First, it has been found that the specific activity of secondarily oligomerized CD95L trimers is 2–3 orders of magnitude higher than those of individual trimers (7, 8). Second, microscopic and biochemical results indicate a tight correlation between CD95 clustering and CD95 signaling (18, 19). Third, the crystal structure of the complex of the CD95 and FADD death domains revealed an asymmetric complex with a 5–7 (CD95 DD) to 5 (FADD DD) stoichiometry arguing for a need of at least two trimeric CD95 complexes for activation of FADD-dependent signaling pathways (20). There is furthermore a variety of reports demonstrating an important contribution of lipid raft association, interaction with the actin cytoskeleton, and internalization to apoptosis induction by CD95 (16, 17). It has been recognized that activation of CD95 is associated with its translocation into the lipid raft-containing detergent-insoluble membrane compartment. Moreover, treatment of cells with drugs interfering with the integrity of lipid rafts diminished CD95-mediated caspase-8 activation and apoptosis (21–25). Palmitoylation of cysteine 199 and a lysine-rich region surrounding this residue have been furthermore identified as signals directing CD95 to the lipid raft-containing compartment (26–28). Noteworthy, CD95 mutants with defects in this region are compromised in apoptosis induction but remained active with respect to the stimulation of non-apoptotic signaling pathways (26). Lipid raft localization of CD95 leads to interaction with ezrin, which links CD95 to the actin cytoskeleton and subsequent internalization (29–31). Interfering with this chain of events inhibits apoptosis induction but again still spares non-apoptotic signaling (30). Remarkably, there is evidence for an auto-amplification loop of lipid raft association of CD95 and caspase-8 activation. Therefore, caspase-8 activation is associated with internalization, and inhibition of the latter attenuates caspase-8 activation, but vice versa caspase-8 inhibition can interfere with lipid raft association of CD95 (29). With respect to the relevance of internalization for CD95-mediated apoptosis, there are contradictory data in the literature, but there is now also evidence for the existence of independent routes of internalization with different relevance for apoptotic CD95 signaling that may resolve some of these inconsistencies (26).

In our study we addressed the very first events in CD95 activation connecting ligand binding and lipid raft-associated caspase-8 activation. Oligomerization of soluble CD95L trimers was found to have no major effect on CD95 occupancy despite showing a strong enhancing effect on apoptotic and non-apoptotic CD95 signaling emphasizing the idea that secondary interaction of initially formed CD95L-CD95 complexes precedes CD95 activation. We further found that CD95 activation precedes the ligand-induced association of CD95 with the lipid raft compartment but, noteworthy, the activated CD95 species not only triggered their own lipid raft association but also those of other inactive CD95 molecules.

EXPERIMENTAL PROCEDURES

Cell Lines, Reagents, and Antibodies—HEK293, HT1080, Jurkat, and A498 cells as well as transfectants derived thereof were maintained in RPMI1640 medium and HaCaT cells in DMEM high glucose (4.5 g/liter) with L-glutamine (PAA, Pasching, Germany), both containing 10% heat-inactivated fetal calf serum (FCS) (PAA). The following cell variants have already been described elsewhere: Jurkat RAPO (32), Jurkat RAPO-CD95L (5), HT1080-FAP (13), HT1080-Bcl2, and HaCaT-Bcl2 (33, 34). Caspase-8 siRNA was purchased from Qiagen (Hilden, Germany), and the pan-caspase inhibitor zVAD-fmk was from Bachem (Weil am Rhein, Germany). Cycloheximide (CHX), iodoacetamide, Pefabloc, NaF, and sodium orthovanadate were obtained from Sigma. The various FLAG-tagged variants of soluble CD95L used in this study were produced in HEK293 cells and purified by affinity chromatography on anti-FLAG mAb M2-agarose (Sigma). Antibodies specific for phospho-IκBα and caspase-3 were purchased from Cell Signaling Technologies (Danvers, MA). Antibodies for IκBα (FL), CD95 (C-20), Bcl2 (C-21), FADD (H-181), and ERK-2 (C-14) were from Santa Cruz Biotechnology (Santa Cruz, CA), and flotillin-2/ESA-, transferrin receptor-, and CD40-specific antibodies from BD Transduction Laboratories™. Anti-tubulin was from Dunn Labortechnik (Asbach, Germany). The fibroblast activation protein (FAP)-specific antibody and the phosphatidylethanolamine-conjugated CD95L-specific antibody were from R&D (Wiesbaden, Germany) and eBioscience (San Diego, CA). The caspase-8 antibody was a gift from Prof. Dr. K. Schulze-Osthoff (University of Tübingen).

Retroviral Infection—DNAs encoding the chimeric CD40-CD95 receptors were cloned into the retroviral vector pLZNGFR-PKG (kind gift of Dr. M. Topp, University of Würzburg) placing them under control of the phosphoglycerate kinase promoter. Upstream of this mouse promoter a truncated

version of the human low affinity nerve growth factor receptor is expressed by the 5′-long terminal repeat of the vector. The retroviral CD40-CD95 constructs were co-transfected in HEK293 cells with the pCL10-A1 packaging plasmid using Lipofectamine (Invitrogen). After 2 days, virus particle-containing supernatants were harvested and filtered (0.4 μM). The next day, HaCaT and HT1080 cells and the virus supernatants were centrifuged for 2 h at 32 °C in the presence of 1 μg/ml Polybrene. After several days, cells were analyzed by FACS analysis for nerve growth factor receptor expression and then immunoselected with anti-Phycoerythrin beads (Milteny Biotech, Bergisch-Gladbach, Germany).

Cell Death Assay—Cells (20×10^3 cells per well) were seeded in triplicate in 96-well tissue culture plates overnight. The next day cells were treated in triplicate with the indicated ligand variants in the presence or absence of CHX (2.5 μg/ml). Oligomerization with the FLAG-tag-specific mAb M2 (1 μg/ml) was arranged for 30 min before use. To analyze the effects of membrane CD95L, RAPO-CD95L cells, and as a control RAPO cells or RAPO cells supplemented with supernatant of RAPO-CD95L cells were used to overlay the previously seeded adherent cells. The concentration of soluble CD95L in the RAPO-CD95L supernatants maximally reached 10 ng/ml (data not shown). Cell viability was in all cases determined after 18 h by crystal violet staining.

Determination of IL8 Production—Cells were seeded in 96-well plates (20×10^3 cells per well) and cultured overnight. The following day medium was changed, and cells were pretreated with CHX (2.5 μg/ml) and zVAD-fmk (20 μM). Thereafter, cells were incubated for 6 h with the indicated CD95L-variants. At the end, supernatants were collected, and IL8 production was determined by enzyme-linked immunosorbent assay (BD Biosciences Pharmingen).

Western Blotting—For preparation of total cell lysates, cells were harvested in ice-cold phosphate-buffered saline (PBS) and centrifuged (3 min, 2300 rpm, 4 °C), and the pellet was directly lysed in 4× Laemmli sample buffer (8% SDS, 10% β-mercaptoethanol, 40% glycerol, 0.2 M Tris, pH 8.0) supplemented with phosphatase inhibitor mixture II (Sigma). Protein samples were boiled for 5 min at 96 °C after 15 s of sonification. For preparation of Triton X-100 lysates, cell pellets were lysed in lysis buffer (30 mM Tris-HCl, pH 7.5, 1% Triton X-100, 10% glycerol, 120 mM NaCl) supplemented with complete protease inhibitor mixture (Roche Diagnostics) for 20 min on ice. Lysates were centrifuged twice (20 min, 14,000 rpm). Samples were separated by SDS-PAGE and transferred to nitrocellulose membranes. Next, nonspecific binding sites were blocked by incubation with Tris-buffered saline containing 0.1% Tween 20 and 5% dry milk. Western blot analyses were performed with primary antibodies of the indicated specificity. For visualization of bound primary antibodies, horseradish peroxidase-conjugated secondary antibodies (Dako, Hamburg, Germany) and the ECL Western blotting detection reagents and analysis system (Amersham Biosciences) were used according to the protocols delivered by the manufacturers. In experiments dedicated to quantitative analysis of relative amounts of proteins, we used fluorescent secondary antibodies (LI-COR, Lincoln, NE) and quantified corresponding protein bands using the LI-COR Odyssey infrared imaging system.

Isolation of Insoluble Membrane Fractions Enriched for Lipid Rafts—To isolate insoluble membrane fractions enriched for lipid rafts, cells (3×10^7) were suspended in 200 μl of RPMI medium and lysed by adding 200 μl of ice-cold Triton X-100 lysis buffer (0.75% Triton X-100 in TNE buffer (25 mM Tris, pH 7.5, 150 mM NaCl, 5 mM EDTA, 1 mM Pefabloc, 5 mM iodoacetamide, 1 mM Na_3VO_4, 1 mM NaF)). Lysates were mixed with 400 μl of 80% sucrose in TNE buffer, transferred in SW60 centrifugation polyallomer tubes (Seton, Los Gatos, CA), and overlaid with 2.8 ml of 30% sucrose in TNE. After centrifugation at 50,000 rpm in a Beckmann SW60 rotor for 20 h at 4 °C, 4 fractions were derived from each sample. The success of separation was controlled by Western blot analysis of flotillin serving as a marker for the detergent-insoluble lipid raft membrane fraction. Moreover, in samples derived from cells treated with GpL fusion proteins, fractions were analyzed via standard luciferase assays.

Binding Studies with Gaussia Princeps Luciferase Fusion Proteins—Cells (2×10^5) were seeded in 24-well plates and cultured overnight. For equilibrium binding studies, cells were first blocked with conventional FLAG-CD95L or Fc-FLAG-CD95L for 30 min at 37 °C. Then cells were treated with the indicated concentrations of one of the GpL-CD95L variants for 1 h at 37 °C. For competitive inhibition experiments, cells were incubated with a mixture of 25 ng/ml (~200 pM) GpL-FLAG-CD95L and the indicated concentrations of conventional FLAG-CD95L. Unbound ligands were removed by 10 washes in ice-cold PBS. Cells were harvested in 50 μl per well in culture medium (0.5% FCS, penicillin/streptomycin) and transferred into a black 96-well plate. Cell-associated luciferase activity was determined using a *Gaussia* luciferase assay kit (New England Biolabs GmbH, Frankfurt a.M., Germany). In brief, 10–25 μl of substrate-buffer solution was given to each well, and light emission was immediately measured for 1 s per sample with a Lucy 2 Luminometer (Anthos Labtec Instruments, Krefeld, Germany). To determine the dissociation rate of GpL-FLAG-CD95L, cells were grown overnight in 24-well culture dishes (2×10^5 cells/well). Half of the cells were blocked with FLAG-CD95L (2 μg/ml) for 30 min at 37 °C, and subsequently all samples were incubated with constant concentrations of GpL-FLAG-CD95L for 1 h at 37 °C to reach equilibrium binding. Cells were then treated for different times with an excess (2 μg/ml) of FLAG-CD95L, and cell-associated luciferase activity was again determined with the *Gaussia* luciferase assay kit. For determination of the association kinetics, cells were again seeded in 24-well plates overnight (2×10^5 cells/well), and the next day half of the samples were blocked with FLAG-CD95L (1.5 μg/ml) to determine nonspecific binding. Cells were then treated with three different concentrations of GpL-FLAG-CD95L for varying times, and finally cell-bound GpL-FLAG-CD95L activity was determined.

Silver Staining—The various affinity-purified recombinant ligands were separated by SDS-PAGE, and gels were subsequently stained by the help of the PageSilver™ Silver Staining kit (Fermentas GmbH, St. Leon-Rot, Germany). In brief, after incubation in fixer 1 (50% ethanol, 10% acetic acid) for 60 min

and 2 times in fixer 2 (30% ethanol) for 20 min, gels were washed twice with deionized water. Then gels were incubated for 1 min with a sensitizing solution and washed again twice with deionized water. After 20 min of staining with staining solution and 2 washes, protein bands were visualized by adding developing solution. When the desired signal intensity was achieved, the developer solution was discarded, and the reaction was terminated by adding stop solution.

Flow Cytometry—Cells were treated with a FITC-conjugated CD95-specific antibody (R&D Systems, Wiesbaden, Germany), phosphatidylethanolamine-conjugated anti-human nerve growth factor receptor (CD271) (BD Biosciences), or a corresponding isotype control antibody for 30 min at 4 °C. For detection of CD40, cells were incubated with anti-CD40 (R&D) and phosphatidylethanolamine-conjugated goat anti-mouse IgG (Sigma). Analyses were done using FACSCalibur (BD Biosciences).

Determination of the Detection Limits of CD95L Fusion Proteins—To determine the lower detection limits of GpL-FLAG-TNC-CD95L and MlL-FLAG-TNC-CD95L, 50-μl samples in 0.5% FCS with decreasing concentrations of the two proteins were transferred into black 96-well plates to measure luciferase activity as described above. The detection limit of SEAP-FLAG-TNC-CD95L (50 μl samples in 0.5% FCS) was determined using the Great EscAPe^{TM} SEAP chemiluminescence kit 2.0 from Clontech (Takara Bio Co., Saint-Germain-en-Laye, France). Relative fluorescence of SNAP-Surface® Alexa Fluor® 647 (New England Biolabs) samples (50 μl in 0.5% FCS) and YFP-FLAG-TNC-CD95L were analyzed using an Infinite® 200 PRO multimode reader (Tecan Group Ltd., Männedorf, Schweiz).

Statistical Analysis—Statistical significance of the differences between experimental variables was assessed with Student's *t* test using GraphPad Prism 5.0 (GraphPad software, Inc.) software. The values shown represent the mean ± S.E. for at least three independent experiments. A difference was considered as significant for $p < 0.05$.

RESULTS

Membrane CD95L Is Superior to Soluble CD95L in Triggering CD95 Lipid Raft Translocation—Initially, we addressed the open question of whether soluble and membrane-bound CD95L differ in their capability to stimulate CD95 translocation into the lipid raft compartment. It has been found that oligomerization of soluble trimeric variants of CD95L results in a 100–1000-fold higher capacity to stimulate CD95-associated signaling pathways (Ref. 8; Fig. 1, *A–C*). A fusion protein of soluble CD95L and the constant region of human IgG1, which assembles into hexameric molecules, also displays high activity comparable with those of oligomerized CD95L trimers (Ref. 7; Fig. 1, *A–C*). Likewise, single chain variable fragment antibody fusion proteins of CD95L display a 2–3 orders of magnitude higher specific activity to induce CD95-mediated cell death upon binding to a cell surface-expressed antigen (Ref. 11–13; Fig. 1*D*). Oligomerization as well as cell surface immobilization of soluble CD95L are considered as means that result in CD95L molecule species that phenocopy membrane-bound CD95L. Thus, we evaluated whether oligomerization or binding to a cell surface antigen has an influence on the ability of soluble CD95L to trigger lipid raft translocation of CD95. We stimulated HT1080 cells with FLAG-CD95L, FLAG-CD95L oligomerized with the FLAG-specific mAb M2, and Fc-FLAG-CD95L and isolated by sucrose density gradient centrifugation the detergent-insoluble membrane fraction, which is enriched for lipid rafts. In the insoluble membrane fractions derived from non-stimulated cells and M2- or FLAG-CD95L-treated cells, there was only a minor fraction of total CD95 (Fig. 1*E*). In contrast, in cells stimulated with oligomerized FLAG-CD95L or Fc-FLAG-CD95L, Western blot analysis revealed a strong redistribution of CD95 into the lipid raft fraction (Fig. 1*E*). Moreover, procaspase-8 (p55/53) and the p43/41 processing intermediate of caspase-8, which is typically generated in the CD95-associated death inducing signaling complex, were also detectable in the insoluble membrane fraction of cells challenged with oligomerized FLAG-CD95L and Fc-FLAG-CD95L (Fig. 1*E*). Principally similar results were obtained when HT1080 and HT1080 transfectants expressing the cell surface antigen FAP were challenged with sc33-FLAG-CD95L, a fusion protein of soluble CD95L with an N-terminal single chain variable fragment domain specific for FAP. Thus, although sc33-FLAG-CD95L failed on the parental HT1080 cells to trigger significant CD95 lipid raft translocation, it stimulated a corresponding response in the FAP transfectants quite well (Fig. 1*F*). To confirm that the use of oligomerized or cell surface-immobilized soluble CD95L as a surrogate for membrane CD95L was permissible, we also analyzed cocultures of HT1080 cells and either the CD95-deficient Jurkat clone RAPO or a transfectant of the latter (RAPO-CD95L) expressing membrane CD95L (Fig. 2*A*). RAPO-CD95L cells, but not RAPO cells, efficiently triggered cell death induction and IL8 production and thus expectedly behaved similar to oligomerized and cell surface-immobilized soluble CD95L (Fig. 2, *B* and *C*). In particular, RAPO cells supplemented with supernatants of RAPO-CD95L cells that contain soluble CD95L released from its membrane-bound precursor were inactive (Fig. 2, *B* and *C*). Likewise, there was only in the cocultures with RAPO-CD95L cells an increase of CD95 in the lipid raft-containing detergent-insoluble membrane fraction (compare #1 fractions in Fig. 2*D*).

In sum, our data indicate that CD95 occupation by soluble CD95L is neither sufficient to trigger efficient activation of CD95-associated signaling pathways nor enough to enrich CD95 in the lipid raft-containing detergent-insoluble membrane fraction.

Avidity Has No Major Effect on CD95 Occupation—Although binding of soluble CD95L trimers to CD95 has been principally demonstrated by FACS and various biochemical means (8), rigorous cellular binding data concerning the interaction of CD95 with soluble CD95L are not available. Thus, it cannot be fully ruled out that the enhanced activity of oligomerized CD95L is due to changes in the kinetic parameters of CD95L-CD95 interaction, such as an avidity-driven increase in apparent affinity or reduced dissociation of ligand-receptor complexes.

To address this issue, we were interested in performing cellular binding studies to correlate CD95 occupancy by CD95L directly with CD95 activity. In corresponding experiments there is a need for a labeled version of CD95L that allows quantification of the cell-bound molecules. Biochemical labeling of CD95L and of TNF ligands in general, for example with iodine or biotin, however, is not necessarily trivial. It can be quite

difficult to define conditions allowing significant and reproducible labeling of a TNF ligand without losing bioactivity. And even if labeling was successful, there is still the intrinsic problem that one obtains a mixture of molecules labeled to a different extent and on different sides, resulting in a heterogeneity that can distort quantitative analysis. To overcome these limitations, we looked for a general method that allows labeling of TNF ligands by genetic engineering and used for this purpose CD95L as a prototypic example. Therefore, we searched for a protein domain that can be genetically fused to CD95L (or other TNF ligands) and that fulfills two criteria. First, the protein domain must not interfere with the activity of the THD, and second the protein domain has to be detectable with high sensitivity and over a wide range of concentrations. It is evident from the literature that TNF ligand fusion proteins in which the THD is N-terminally fused to other protein domains often show normal undisturbed receptor binding (35). We, therefore, constructed and analyzed CD95L fusion proteins with N-ter-

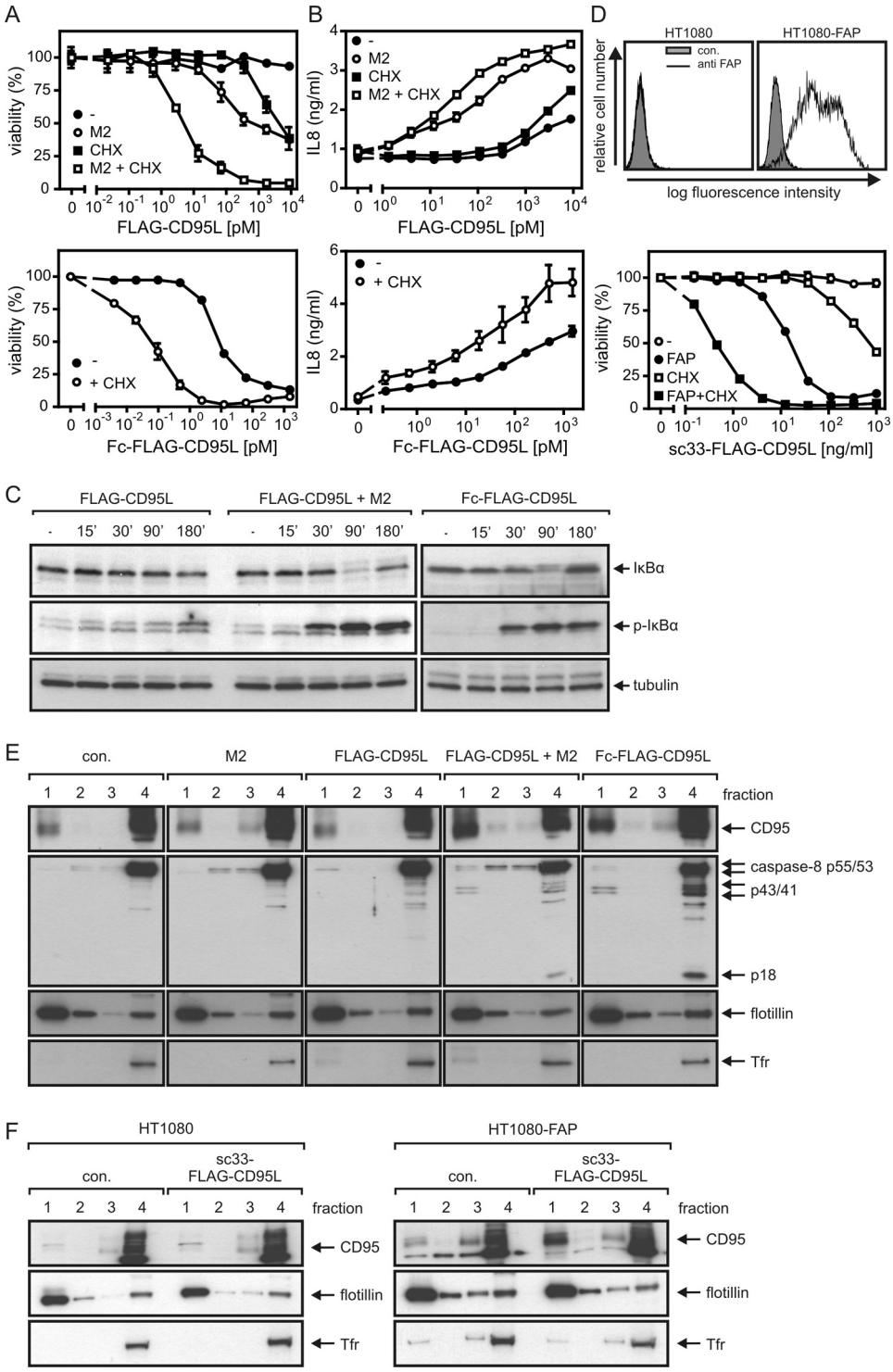

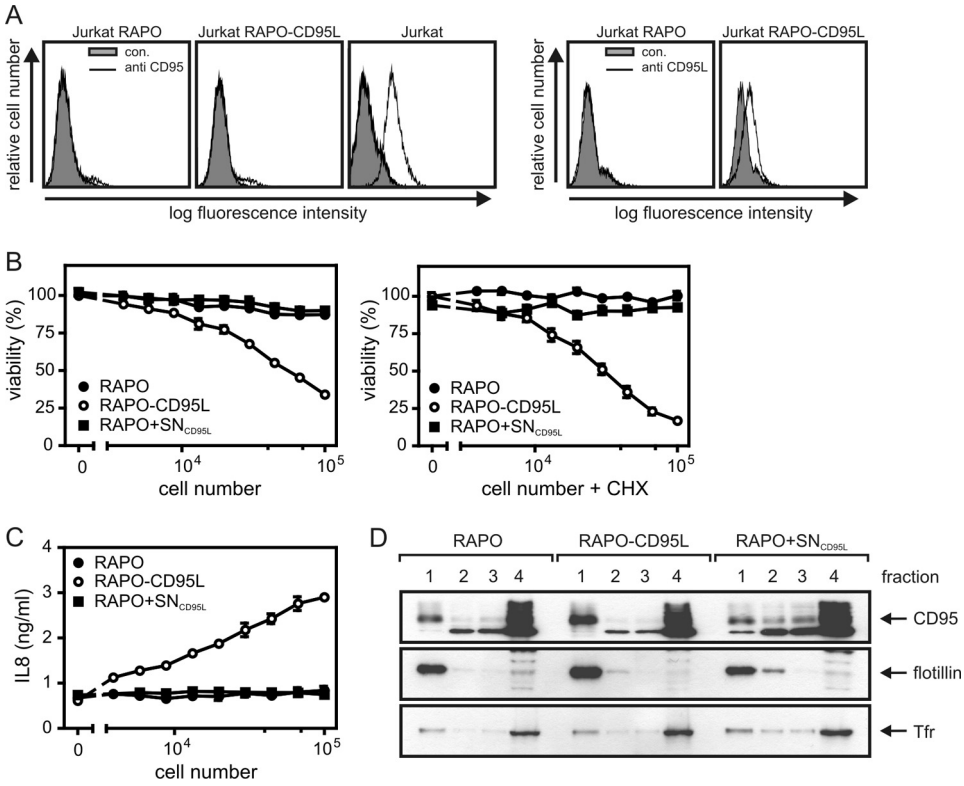

FIGURE 2. **Cells expressing membrane-bound CD95L induce efficient CD95 translocation into lipid rafts.** *A*, FACS analysis of CD95 and CD95L expression of the CD95-deficient Jurkat RAPO clone and a membrane-CD95L-expressing transfectant derived thereof. *B* and *C*, HT1080 cells (2×10^4 cells/well) were seeded in 96-well plates. The next day, medium was replaced by medium containing the indicated amounts of RAPO or RAPO-CD95L cells. As an additional control RAPO cells suspended in supernatant of RAPO-CD95L cells (*RAPO+SN$_{CD95L}$*) was used. Cell death induction (*B*) was analyzed in the presence and absence of CHX measuring cell viability after 18 h using crystal violet staining. To determine IL8 production, supernatants were analyzed by ELISA (*C*). *D*, HT1080 cells were cocultivated for 4 h with RAPO, RAPO-CD95L cells, and again RAPO cells supplemented with supernatant of RAPO-CD95L cells containing soluble CD95L (*RAPO+SN$_{CD95L}$*). Triton X-100 lysates of the various cocultures were then fractionated by sucrose density gradient centrifugation, and fractions were analyzed by Western blotting for the presence of CD95. The upper fraction (*1*) again contained the insoluble membrane fraction with lipid rafts, and soluble proteins were again present in *fraction 4*.

minal *G. princeps* luciferase (GpL; Ref. 36), *Metridia longa* luciferase (MlL), secreted alkaline phosphatase (SEAP), yellow fluorescent protein (YFP), and an O^6-alkylguanine-DNA-alkyltransferase-based SNAP tag as reporter domains. We recently observed that the integrity of the trimeric nature of some soluble TNF ligands benefits from the N-terminal fusion of the small (~3 kDa) trimerization domain of tenascin-C (37, 38). We, therefore, included this domain also in our fusion proteins between the reporter domain (including a FLAG tag) and the THD. All fusion proteins were secreted in the supernatant of transiently transfected HEK293 cells. Although GpL-FLAG-TNC-CD95L, SNAP-FLAG-TNC-CD95L, and SEAP-FLAG-TNC-CD95L typically reached concentrations of 0.5–1.5 μg/ml after 4–5 days of culture, the productivity of YFP-FLAG-TNC-CD95L and MlL-FLAG-TNC-CD95L was rather low (~0.1 μg/ml). Bioluminescent detection of 50-μl samples of GpL-FLAG-TNC-CD95L, MlL-FLAG-TNC-CD95L, and SEAP-FLAG-TNC-CD95L was possible down to concentrations

FIGURE 1. **Highly active oligomerized trimers of soluble CD95L, hexameric CD95L, and a cell surface antigen-bound soluble CD95L fusion protein but not barely active CD95L trimers induce efficient CD95 translocation into lipid rafts.** *A*, HT1080 cells (2×10^4 per well of a 96-well plate) were stimulated in triplicate with the indicated concentrations of FLAG-CD95L, anti-FLAG mAb M2 oligomerized FLAG-CD95L, and Fc-FLAG-CD95L in the presence and absence of 2.5 μg/ml CHX overnight, and cell viability was finally determined by crystal violet staining. For FLAG-CD95L oligomerization, 1 μg/ml mAb M2 were used irrespective of the applied FLAG-CD95L concentration. To calculate the percentage of viability, measured data were corrected for background staining of completely killed cells (0% viability) according to a group where cells have been treated with a "killing mixture" containing 80 μg/ml CHX and high doses of Fc-FLAG-CD95L. *B*, HT1080 cells were seeded in 96-well plates (2×10^4 cells/well) and treated the next day with the indicated combinations of FLAG-CD95L, anti-FLAG mAb M2-oligomerized FLAG-CD95L, and Fc-FLAG-CD95L and CHX (2.5 μg/ml) in the presence of zVAD-fmk (20 μM) for 6 h. Cell culture supernatants were then collected to determine the IL8 content by ELISA. CHX treatment served to enhance CD95 signaling, and zVAD-fmk was added to prevent apoptosis induction, which otherwise would counteract IL8 production. Prior stimulation cell culture medium was changed to minimize the background of constitutively expressed IL8. *C*, HT1080 cells were stimulated for the indicated times with 200 ng/ml (~3400 pM) of FLAG-CD95L, anti-FLAG mAb M2-oligomerized FLAG-CD95L, Fc-FLAG-CD95L (~ 600 pM), and total cell lysates were analyzed by SDS-PAGE and Western blotting for the presence of the indicated proteins. Cells were again pretreated with CHX to enhance CD95 signaling, and zVAD-fmk was again used to block apoptosis induction. *D*, HT1080 cells and HT1080-FAP transfectants (FACS analysis, *upper panel*) were challenged with the indicated concentrations of the FAP-interacting single chain variable fragment -CD95L fusion protein sc33-FLAG-CD95L in the presence and absence of CHX (2.5 μg/ml), and cell viability was determined the next day by crystal violet staining (*lower panel*). *E*, HT1080 cells were stimulated as indicated with the various CD95L variants (200 ng/ml) for 2 h and were then subjected to cell fractionation by Triton X-100 lysis and sucrose density gradient centrifugation. The upper fraction (*1*) with the lowest sucrose density contained the insoluble membrane fraction including lipid rafts, whereas the soluble proteins were present in fraction *4*. Fractions were analyzed by Western blotting for the presence of the indicated proteins. Flotillin served as marker for the lipid raft fraction. *F*, HT1080 and HT1080-FAP cells were stimulated with sc33-FLAG-CD95L (200 ng/ml, 1.5 h) or remained untreated as a control. Compartmentation of the indicated proteins was then analyzed as described in *E*. *Tfr*, transferrin receptor.

<1 fM (~10^{-4} ng/ml) with GpL-FLAG-TNC-CD95L showing a somewhat higher traceability than MlL-FLAG-TNC-CD95L and SEAP-FLAG-TNC-CD95L (Fig. 3*A*). The sensitivity of fluorescent detection of YFP-FLAG-TNC-CD95L and the Alexa-647 SNAP-tag label for the SNAP-FLAG-CD95L fusion protein by far did not reach the sensitivity of the bioluminescent constructs. GpL-FLAG-TNC-CD95L elicited only a very weak cytotoxic activity that was 100-fold increased upon oligomerization using the FLAG-specific mAb M2 (Fig. 3*B*). Thus, it behaved like conventional soluble CD95L trimers. In contrast, all other constructs showed high cytotoxic activity irrespective of anti-FLAG treatment, indicating significant aggregation of trimeric CD95L molecules (Fig. 3*B*). In sum, the GpL-FLAG-TNC-CD95L fusion protein showed the best traceability, good productivity, and no unwanted aggregation. We used therefore for our following studies GpL fusion proteins of Flag-CD95L and Fc-Flag-CD95L. The corresponding fusion proteins were designated in the following as GpL-FLAG-CD95L and GpL-Fc-FLAG-CD95L (Fig. 3*C*). All CD95L variants were purified by affinity chromatography on anti-FLAG-agarose to homogeneity (Fig. 3*D*). Side-by-side analysis of the GpL-CD95L fusion proteins and their corresponding conventional CD95L variants confirmed again that the presence of the GpL reporter domain has no major impact on the CD95 stimulating capacities of the CD95L domain (Fig. 3, *E* and *F*). Thus, the GpL reporter domain neither interfered with the anti-FLAG oligomerization-induced increase in the activity of trimeric FLAG-CD95L nor with the already high activity of hexameric CD95L (Fig. 3, *E* and *F*) which cannot be further increased by oligomerization.

Apoptosis induction by CD95 receptor is triggered by the autocatalytic processing of receptor-associated dimers of procaspase-8 to mature caspase-8 heterotetramers. The latter cleaves and thereby activates effector caspases that execute the apoptotic effector phase. Cells in which this sequence of events is sufficient to induce apoptosis are designated as type I cells. However, there are also cells in which effector caspase processing by caspase-8 is inefficient and where robust triggering of CD95-mediated apoptosis, therefore, requires an amplification mechanism. In such so called type II cells, caspase-8 processes BH3-interacting domain death agonist, a proapoptotic member of the Bcl2 family, leading to the release of a BH3-interacting domain death agonist fragment that stimulates the release of proapoptotic factors from mitochondria that cooperate with caspase-8 in the activation of effector caspases. The mitochondria-derived factors antagonize the action of the effector caspase inhibitory inhibitor of apoptosis proteins (*e.g.* SMAC) but also stimulate activation of procaspase-9 (*e.g.* cytochrome *c*), another type of initiator caspase. Although the difference between type I and type II cells has mainly been attributed to the expression status of IAP proteins in recent years, there is also evidence that these two categories of cells differ in the mechanisms of CD95 activation (39, 40). As type II cells depend on the mitochondrial pathway for strong apoptosis induction, expression of Bcl2, an antiapoptotic member of the Bcl2 family acting downstream of BID, can protect these cells from CD95-induced cell death (Fig. 4, *A* and *B*). In contrast, CD95L-challenged type I cells do not benefit from Bcl2 expression (Fig. 4, *A* and *B*). We performed binding studies with HT1080 and A498 cells, which are type II as well as with HaCaT cells which are type I (Fig. 4, *A* and *B*). A498 cells were included due to their use in some of the later experiments. HT1080 and A498 cells displayed roughly similar CD95 cell surface expression, whereas the expression on HaCaT cells was significantly lower but still clearly evident (Fig. 4*C*). Equilibrium binding studies with GpL-FLAG-CD95L on HT1080, HaCaT, and A498 cells yielded K_D values between 2000 (~240 ng/ml) and 3600 pM (~430 ng/ml) (Fig. 4*D*). Notably, the affinities between anti-FLAG-oligomerized GpL-FLAG-CD95L and CD95 and GpL-Fc-FLAG-CD95L and CD95 were comparable or a bit lower compared with the interaction of CD95 and GpL-FLAG-CD95L (Fig. 4*D*, Table 1). Thus, increasing the avidity of the interaction between CD95L trimers and CD95 had no or only a very minor effect on ligand occupancy of CD95. When conventional FLAG-CD95L was used as an inhibitor of GpL-FLAG-CD95L binding in homologous competitor experiments, K_i values between 1000 and 840 pM were obtained in HT1080, HaCaT, and A498 cells (Fig. 4*E*). The K_i values for FLAG-CD95L obtained in these experiments are identical to the K_D of this molecule for CD95. The K_D values determined this way for conventional FLAG-CD95L are in good accordance with the values obtained by equilibrium binding studies with GpL-FLAG-CD95L (Fig. 4*D*, Table 1) and emphasize the fact that N-terminal tagging of soluble CD95L variants with a GpL domain does not interfere with the functionality of the THD domain of CD95L.

The dissociation and association rate constants of the interaction of GpL-FLAG-CD95L and CD95 were also determined for HT1080 and HaCaT cells. To quantify dissociation, cells were loaded with 25 ng/ml GpL-FLAG-CD95L and were subsequently chased with an excess of FLAG-CD95L to prevent rebinding of dissociated GpL-FLAG-CD95L molecules. Specific binding was then determined as a function of time and used to calculate the dissociation rate constant (k_{off}). For HT1080 cells, this way we determined a k_{off} of 1.0×10^{-3} s^{-1} corresponding to a half-life of 12.4 min and for HaCaT cells a k_{off} of 1.5×10^{-3} s^{-1} (half-life, 8.1 min) (Fig. 4*F*, Table 2). An association rate constant (k_{on}) of 2.9×10^5 $M^{-1}s^{-1}$ for HT1080 cells and 1.7×10^5 $M^{-1}s^{-1}$ for HaCaT cells were obtained by determination of the association kinetics of GpL-FLAG-CD95L at three constant concentrations (Fig. 4*G*, Table 2). The K_D values of the interaction of GpL-FLAG-CD95L and CD95 that were calculated from the k_{off} and k_{on} values are again in good accordance with the corresponding values determined before by equilibrium binding studies and homologous competitor experiments (Fig. 4, *D* and *E*; Table 1).

Oligomerization of soluble CD95L is necessary to enhance association of CD95 with the lipid raft-containing membrane compartment (Fig. 1*E*). Accordingly, the distribution of GpL activity between the lipid raft-containing fraction 1 and the soluble fraction 4 obtained after sucrose density gradient centrifugation shifted in favor of fraction 1 for oligomerized GpL-FLAG-CD95L and especially GpL-Fc-FLAG-CD95L (Fig. 5). Thus, the use of GpL-FLAG-CD95L or GpL-Fc-FLAG-CD95L as tracers confirmed that receptor binding of soluble, poorly active CD95L is insufficient to change the lipid raft-non-raft distribution of CD95.

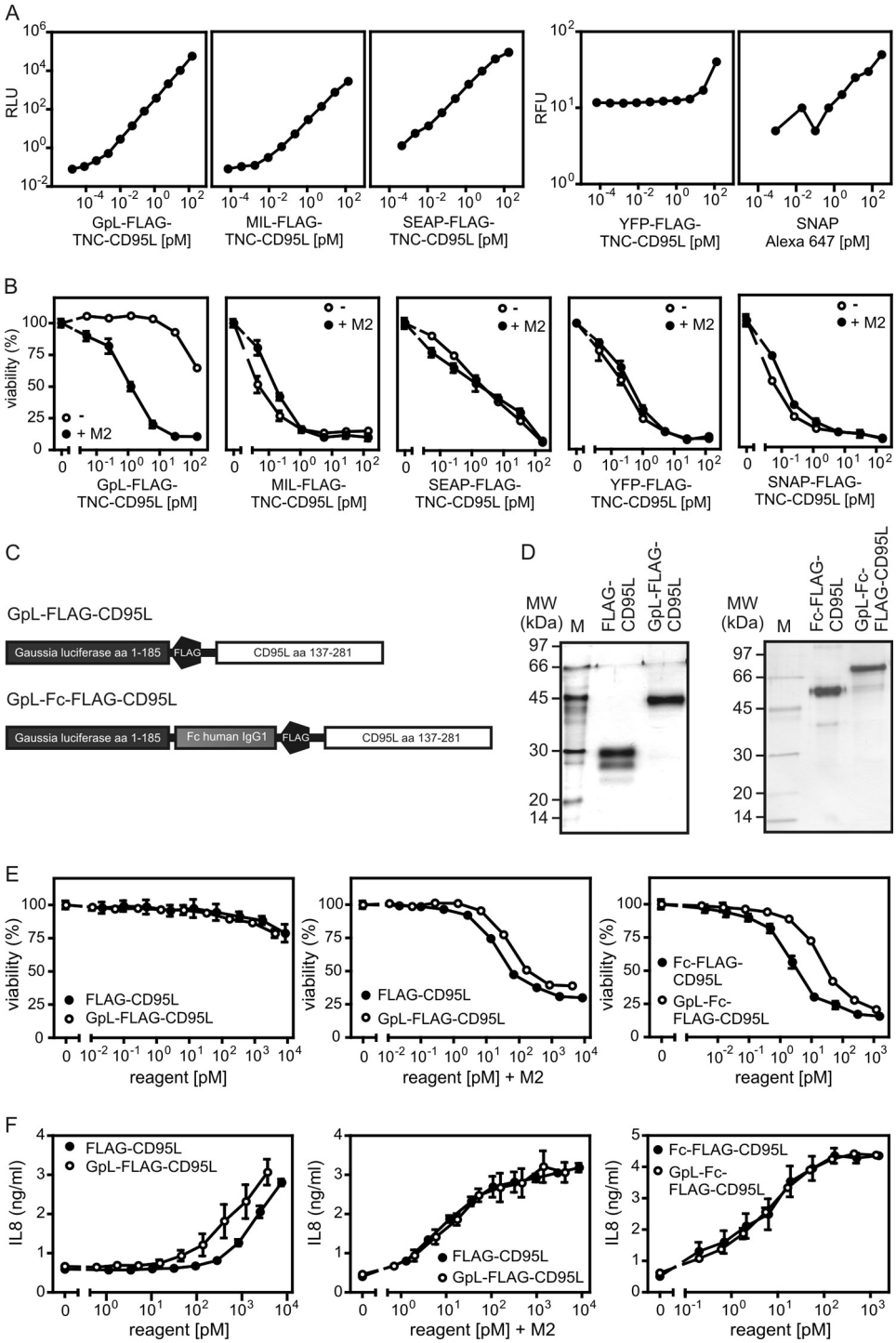

FIGURE 3. **Sensitivity and biological activity of various N-terminal-labeled CD95L fusion proteins.** *A*, bioluminescence of decreasing concentrations of CD95L fusion proteins with N-terminal *GpL*, MIL, and SEAP have been detected using a *Gaussia* luciferase assay kit. Fluorescence of the YFP fusion protein of CD95L and the Alexa-647 SNAP-tag label, the fluorescent compound dedicated for labeling of SNAP-FLAG-TNC-CD95L, was determined at 488 and 633 nm. *RLU*, relative light units; *RFU*, relative fluorescence units. *B*, HT1080 cells were grown overnight (2×10^4 cells per well in a 96-well plate) and were treated the next day in triplicates with the indicated concentrations of the various CD95L fusion proteins and 2.5 μg/ml CHX. This happened with or without oligomerization with the anti-FLAG mAb M2 (1 μg/ml, 30 min prior stimulation). The next day cell viability was measured by crystal violet staining. *C*, shown is domain architecture of GpL-FLAG-CD95L and GpL-Fc-FLAG-CD95L. *D*, 100 ng of the indicated anti-FLAG affinity-purified proteins were separated by SDS-PAGE and visualized by silver staining. Molecular masses (kDa) of prestained marker proteins are indicated. *E* and *F*, HT1080 cells (2×10^4 per well) were seeded in 96-well plates and were stimulated the next day in triplicate with increasing concentrations of FLAG-CD95L, Fc-FLAG-CD95L, GpL-FLAG-CD95L, and GpL-Fc-FLAG-CD95L. Where indicated, FLAG-CD95L and GpL-FLAG-CD95L were oligomerized before stimulation with anti-FLAG mAb M2 (1 μg/ml). Cells that were scheduled for viability analysis were analyzed after 18 h with respect to viability by crystal violet staining (*E*). In samples dedicated for analysis of CD95L-induced production of IL8 (*F*), cell culture medium was changed before stimulation with medium containing 2.5 μg/ml CHX and 20 μM zVAD-fmk to reduce background caused by constitutive IL8 expression and to prevent apoptosis. IL8 content of the supernatants was then determined by ELISA after 6 h.

Activated CD95 Triggers Caspase-8-mediated Lipid Raft Translocation of Non-activated CD95 Molecules—It has been shown that an auto-amplification loop of CD95-induced activation of caspase-8 and caspase-8-driven translocation of CD95 into the lipid raft-containing membrane compartment contributes to the redistribution of CD95 from the soluble to the insoluble membrane compartment (29). However, it is unclear whether this effect is related to an increased retention of active CD95L-CD95-FADD-caspase-8 complexes in the lipid raft-containing membrane compartment or whether this effect also involves a redistribution of inactive CD95 complexes. To have the opportunity to consider the effect of

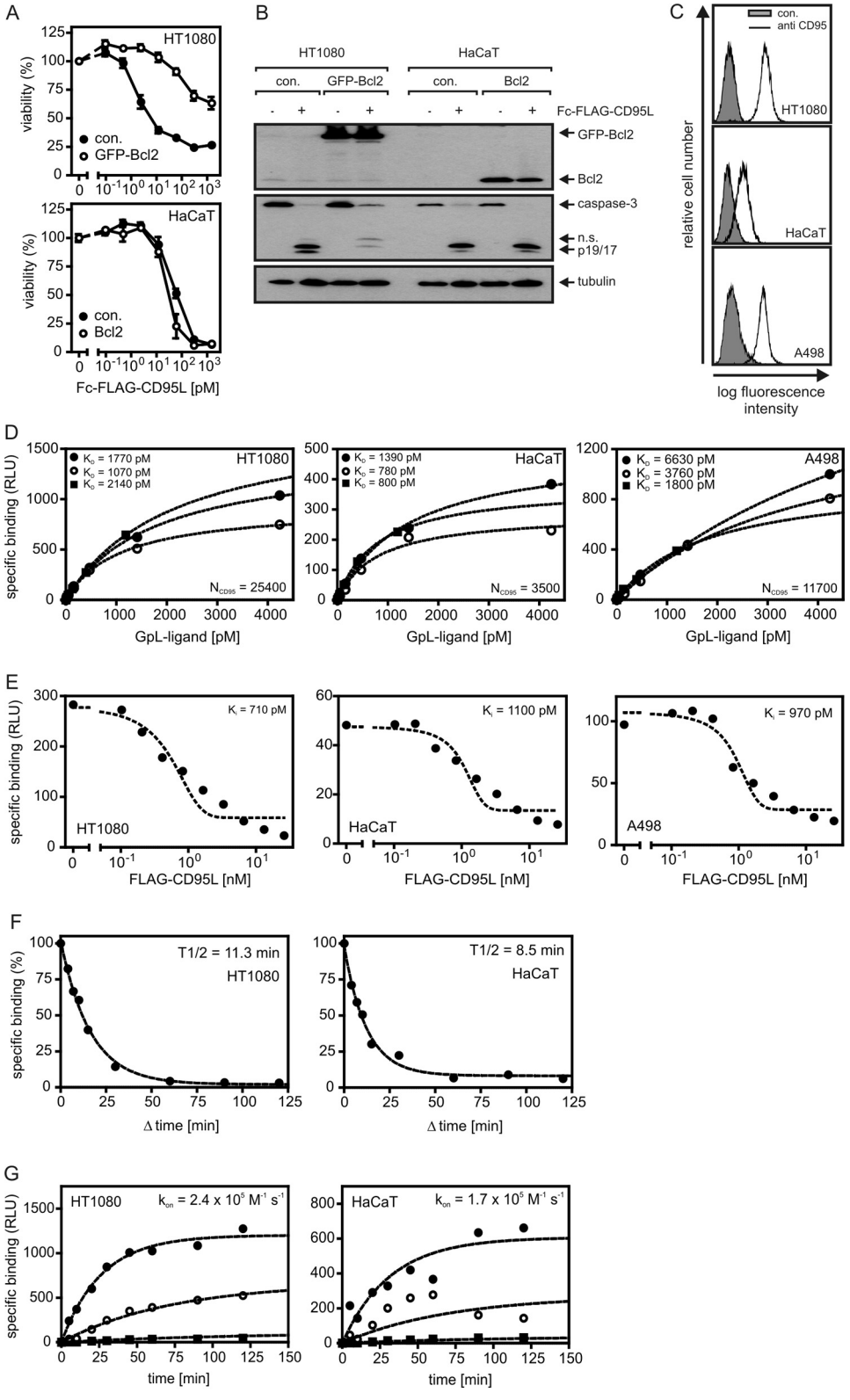

TABLE 1

K_D values of CD95 interaction with trimeric and oligomeric variants of soluble CD95L

	GpL-FLAG-CD95L				GpL-FLAG-CD95L + M2		GpL-Fc-FLAG-CD95L	
	Equilibrium binding		Homologous competition assay		Equilibrium binding		Equilibrium binding	
Cell line	K_D	R^2	K_i	R^2	K_D	R^2	K_D	R^2
HT1080	2000 ± 720	0.996- 0.999	840 ± 90	0.926–0.936	1200 ± 110	0.999–0.998	2600 ± 300	0.999–0.999
HaCaT	2600 ± 1500	0.998- 0.999	850 ± 110	0.943- 0.962	1250 ± 280	0.978–0.997	1500 ± 350	0.99–0.999
A498	3600 ± 1780	0.994- 0.999	1000 ± 20	0.907- 0.945	3000 ± 500	0.998–0.998	1800 ± 660	0.995–0.995

TABLE 2

Kinetic parameters of the interaction of soluble CD95L and cellular CD95

Cell line	K_D of GpL-FLAG-CD95L[a]	Binding sites per cell	K_D of FLAG-CD95L[b]	K_{off}[c]	K_{on}[d]	$K_D = K_{off}/K_{on}$
	pM		pM	s^{-1}	$M^{-1}s^{-1}$	pM
HT1080	2000 ± 720	23000 ± 7900	840 ± 90	1.0×10^{-3}	2.9×10^5	3320
HaCaT	2600 ± 1500	4600 ± 2600	850 ± 120	1.5×10^{-3}	1.7×10^5	8740

[a] Derived from equilibrium binding study. $n = 3$.
[b] Derived from homologous competition assay. $n = 3$.
[c] $n = 3–4$ experiments.
[d] $n = 3–4$ experiments.

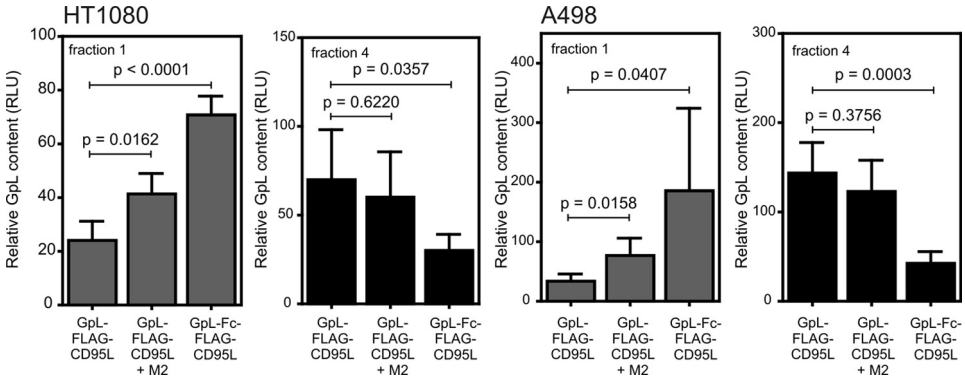

FIGURE 5. **Oligomerization of soluble CD95L trimers triggers enhanced association of CD95 with the lipid raft-containing membrane compartment.** A498 and HT1080 cells were treated for 3–5 h with 1700 pM GpL-FLAG-CD95L and anti-FLAG oligomerized GpL-FLAG-CD95L and 480 pM GpL-Fc-FLAG-CD95L. Cells were lysed in Triton X-100 buffer and further resolved by sucrose density gradient centrifugation. The upper fraction (*1*) again contained the insoluble membrane fraction with lipid rafts, and soluble proteins resided in *fraction 4*. The average amount of the various GpL fusion proteins in *fraction 1* and *4* of 3–5 independent experiments are shown. Please note: high sucrose concentrations and Triton X-100 attenuate the activity of GpL. GpL activities derived from fraction 1 and 4 are thus not directly comparable. *RLU*, relative light units.

an activated species of CD95-associated signaling complexes on inactive non-stimulated CD95 molecules, we stably transfected HT1080 and HaCaT cells with an expression plasmid encoding a chimeric receptor in which the extracellular domain of CD95 has been replaced by the corresponding part of CD40 (Fig. 6, *A* and *B*). We also established transfectants expressing a variant of the chimeric CD40-CD95 receptor bearing a V238N mutation in the CD95 intracellular domain (Fig. 6, *A* and *B*). The V238N mutation corresponds to the murine lpr^{cg} mutation and impairs the capability of CD95 to form a caspase-8 activating complex with FADD and procaspase-8 (41). As CD40L does not interact with CD95 and vice versa CD95L fails to bind CD40 (42), CD95 and CD40-CD95 can independently be stimulated using Fc-FLAG-CD95L and Fc-FLAG-CD40L. In each panel of cells (vector-, CD40-CD95-, and CD40-CD95$_{(V238N)}$-

FIGURE 4. **Cellular binding studies with GpL-tagged CD95L variants.** *A*, HT1080 and HaCaT cells and the corresponding transfectants stably expressing Bcl2-GFP or Bcl2 were seeded in 96-well plates (2×10^4 per well) and cultured overnight. The next day cells were stimulated with increasing concentrations of Fc-FLAG-CD95L. After 18 h cell viability was determined via crystal violet staining. *B*, HT1080 and HaCaT cells and their corresponding Bcl2 transfectants were treated with 200 ng/ml Fc-FLAG-CD95L or remained untreated. After 3 h cells were harvested, and Triton X-100 lysates were separated by SDS-PAGE and analyzed by Western blotting for the indicated proteins. *n.s.*, not significant. *C*, FACS analysis of cell surface expression of CD95 is shown. *D*, equilibrium binding studies with GpL-FLAG-CD95L (*filled circles*), anti-FLAG oligomerized GpL-FLAG-CD95L (*open circles*), and GpL-Fc-FLAG-CD95L (*filled squares*) were performed for the indicated cell lines as described under "Experimental Procedures." CD95 numbers per cell (N_{CD95}) calculated from the experiments shown are indicated. *E*, for homologous competition experiments, cells were incubated in 24-well plates for 2 h at 37 °C with 200 pM (~25 ng/ml) GpL-FLAG-CD95L and the indicated concentrations of conventional FLAG-CD95L. Unbound ligand was then removed by 10 washes with ice-cold PBS, and remaining cell associated luciferase activity was determined. *F*, cells were cultivated in a 24-well plate (2×10^5 cells/well). Half of the wells were pretreated with FLAG-CD95L (0.5 h, 2 μg/ml) to block CD95-pecific binding. Cells of all wells were then incubated for 1 h with 25 ng/ml (~ 200 pM) of GpL-FLAG-CD95L. To determine dissociation as a function of time, 2 μg/ml FLAG-CD95L were added for the indicated time intervals to blocked and non-blocked samples. Cell associated luciferase activity was determined, and remaining specific binding was calculated for all time points as the difference of blocked and non-blocked samples. *G*, untreated and FLAG-CD95L-blocked (0.5 h, 1.5 μg/ml) cells were incubated with GpL-FLAG-CD95L (2100 (*filled circles*), 420 (*open circles*), and 40 pM (*filled squares*)) for the indicated times, and specific binding was calculated again as the difference of total (non-blocked samples) and unspecific (blocked samples) binding. The GraphPad Prism5 software was used to fit the association kinetics to obtain the association rate constant. *RLU*, relative light units.

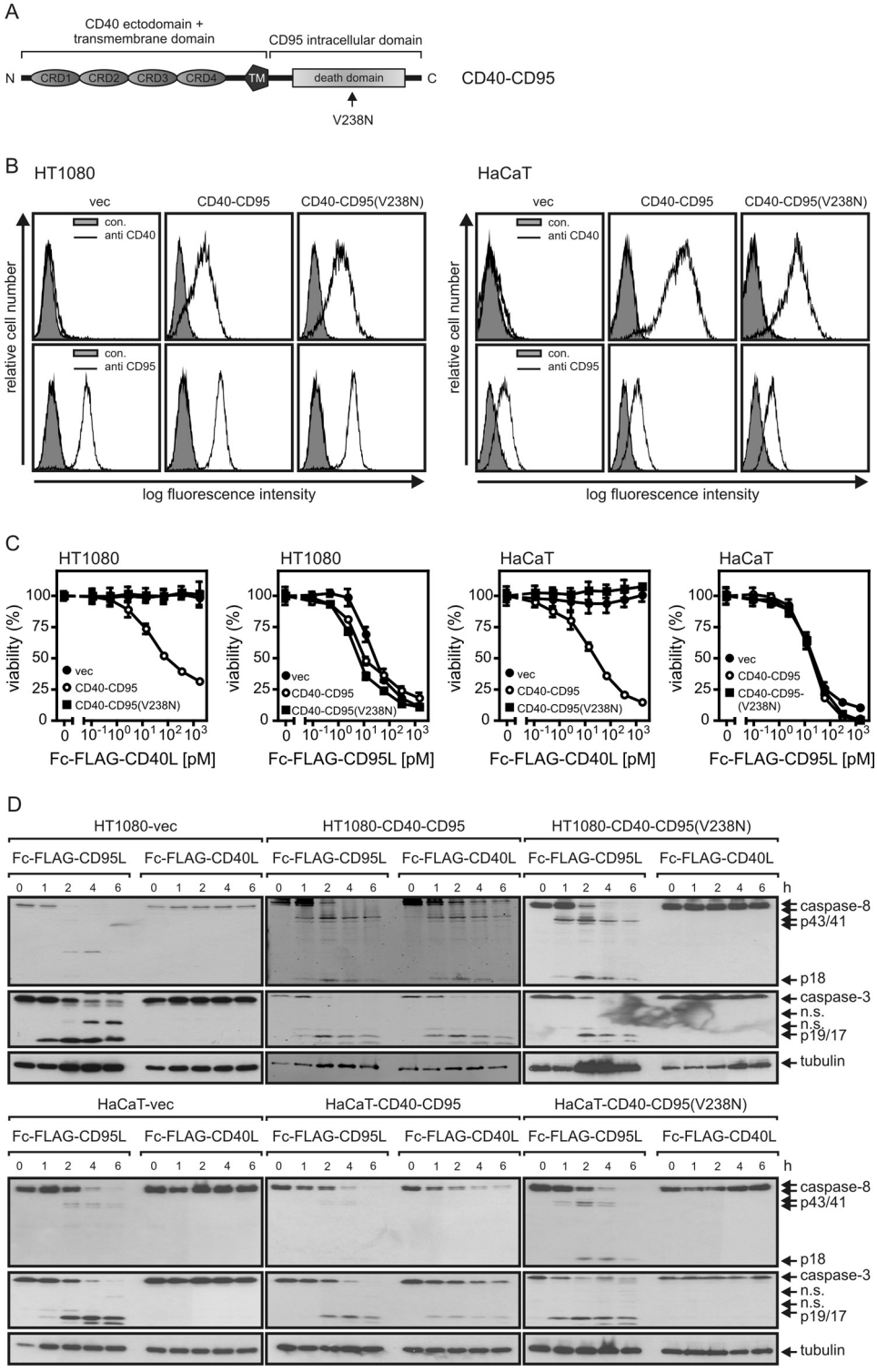

FIGURE 6. **Activation of CD95-associated signaling pathways by chimeric CD40-CD95 receptors.** *A*, shown is domain architecture of CD40-CD95 and CD40-CD95$_{(V238N)}$. The *black arrow* indicates the point mutation on amino acid position 238 in the CD95 death domain. *CRD*, cysteine rich domain; *TM*, transmembrane domain. *B*, cell surface expression of endogenous CD95 and chimeric CD40-CD95/CD40-CD95$_{(V238N)}$ receptors were analyzed in the indicated cell lines by help of CD95- and CD40-specific antibodies. *C*, the indicated cell lines (2×10^4 cells per well of a 96-well plate) were challenged in triplicate with increasing concentrations of Fc-FLAG-CD40L and Fc-FLAG-CD95L. After 18–24 h cell viability was determined by crystal violet staining. *D*, the various cell lines were stimulated for the indicated times with Fc-FLAG-CD40L (200 ng/ml) and Fc-FLAG-CD95L (200 ng/ml). Total cell lysates were separated by SDS-PAGE and analyzed by Western blotting for the presence/processing of the indicated proteins. *n.s.*, not significant.

transfected), cell death was induced with the same dose-response relationship by Fc-FLAG-CD95L (Fig. 6*C*). In contrast, Fc-FLAG-CD40L only triggered cell death in the CD40-CD95 expressing cells but showed no effects on vector or CD40-CD95$_{(V238N)}$ transfectants (Fig. 6*C*). Likewise, Fc-FLAG-CD95L triggered caspase processing in all cells,

whereas Fc-FLAG-CD40L did this only in the CD40-CD95 but not in the vector or CD40-CD95$_{(V238N)}$ transfectants (Fig. 6*D*).

Stimulation of CD40-CD95 resulted in the enrichment of this molecule in the lipid raft-containing membrane fraction as found before for endogenous wild-type CD95 (Fig. 7, *A* and *B*). In further accordance with the finding that CD95 "activity," thus triggering of CD95-associated signaling, is necessary for robust lipid raft translocation, we observed no or only a minor shift of CD40-CD95$_{(V238N)}$ into the lipid raft fraction upon treating the corresponding transfectants with Fc-FLAG-CD40L (Fig. 7, *A* and *B*). Stimulation of endogenous CD95 with Fc-FLAG-CD95L, thus activation of CD95-associated signaling pathways, led to a significant redistribution of the chimeric

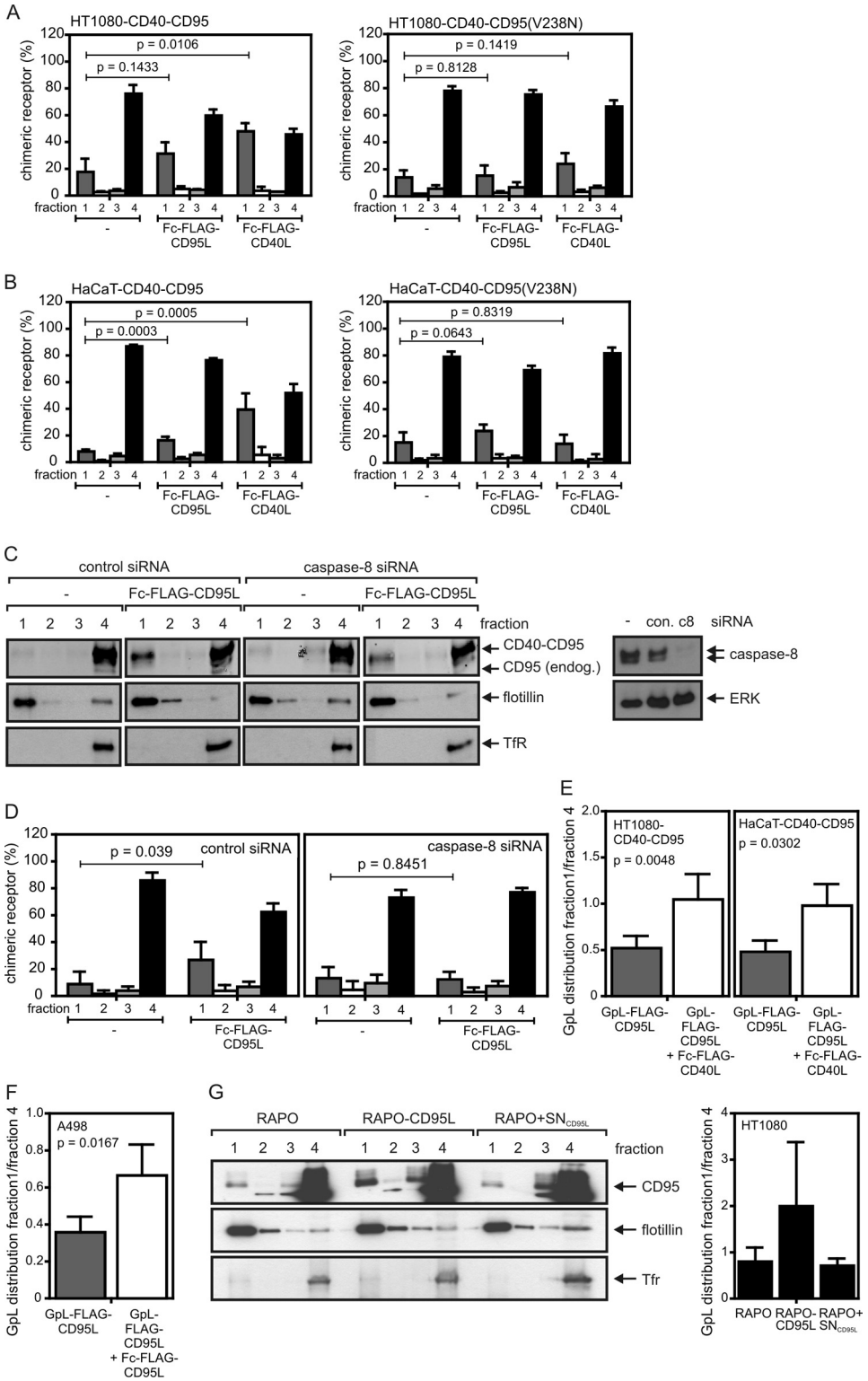

receptor into the lipid raft fraction, suggesting that "activated" CD95 molecules enhance the association of unliganded inactive receptors with the lipid raft compartment (Fig. 7, *A* and *B*). Notably, this effect was inhibited by knockdown of caspase-8 (Fig. 7, *C* and *D*). To further evaluate whether inactive endogenous CD95 also shifts into the lipid raft fraction upon triggering of CD95-associated signaling pathways, we took advantage of the fact that GpL-FLAG-CD95L trimers bind to CD95 without triggering lipid raft association and activation of intracellular signaling (Figs. 1*E* and 5). Therefore, we loaded the CD40-CD95 expressing cells with GpL-FLAG-CD95L as a tracer and analyzed its distribution in non-stimulated and Fc-FLAG-CD40L-stimulated cells. There was a significant shift of GpL activity into the lipid raft-containing fraction 1 of sucrose density gradients upon stimulation of cells with Fc-FLAG-CD40L, indicating that "inactive" complexes of CD95 and GpL-FLAG-CD95L shifted indeed into the lipid raft compartment under these conditions (Fig. 7*E*). A similar redistribution of inactive complexes of endogenous CD95 and GpL-FLAG-CD95L was observed when the latter was applied with non-saturating concentrations and if concomitantly the remaining freely accessible CD95 molecules were activated by help of Fc-FLAG-CD95L (Fig. 7*F*). Moreover, cocultivation with the membrane CD95L expressing CD95-deficient RAPO-CD95L cells (Fig. 2) resulted not only in CD95 translocation into the lipid raft containing fraction (Fig. 7*G*, *left panel*) but also triggered the translocation of the GpL-FLAG-CD95L tracer molecules (Fig. 7*G*, *right panel*).

Activation of a Very Small Fraction of Cell Surface-expressed CD95 Can Be Sufficient to Trigger Robust Cell Death—In many studies cells were sensitized for CD95-mediated apoptosis by co-treatment with CHX. The sensitizing effect of this treatment is mainly related to the down-regulation of FLIP proteins that interfere with CD95-associated caspase-8 activation (Refs. 43–46 and supplemental Fig. S1). To recognize a possible effect of cycloheximide treatment on CD95L-CD95 interaction, we performed binding studies with GpL-Fc-FLAG-CD95L in the absence and presence of CHX (Fig. 8*A*). There were no major differences in ligand binding between untreated and CHX-primed cells, indicating that the effect of CHX on CD95-mediated apoptosis is indeed dominantly confined to intracellular mechanisms. Noteworthy, even cell lines where the whole population can be killed by Fc-FLAG-CD95L often show a dramatic decrease in the ED_{50} value for apoptosis induction upon CHX treatment, suggesting that activation of a minor subfraction of cellular CD95 can be fully sufficient to kill cells. To estimate the minimum number of CD95 signaling complexes required for apoptosis induction, we correlated CD95 occupancy and apoptosis induction by GpL-Fc-FLAG-CD95L in CHX-primed and thus maximally sensitized cells. In CHX-sensitized HT1080 and HaCaT cells on average only 0.1 and 2.5% of the cell surface-expressed CD95 molecules had to be liganded with GpL-Fc-FLAG-CD95L to kill half of the cells (Fig. 8*B*). This corresponds on an astonishingly low number of on average 4- and 40-activated receptors per cell.

DISCUSSION

If one defines CD95 to be active when this molecule is in a state where it stimulates intracellular signaling pathways, CD95 activation is not an instantaneous consequence of ligand binding. There is instead evidence that a chain of events is required to place initially formed CD95L-CD95 complexes in a position to engage signaling. Although some details are debated with respect to their general relevance in all cell types, the following events appear distinguishable in the course of CD95 activation: first, binding of CD95L to preassembled inactive CD95 molecules; second, formation of SDS-stable CD95 microaggregates; third, caspase activity-independent assembly of CD95-associated signaling protein oligomerization transduction structures (SPOTS); fourth, CD95 association with lipid rafts; fifth, formation of supramolecular clusters; and last, interaction with the cytoskeleton along with internalization (17, 47, 48). In sum, the mechanisms that have implicated in CD95 activation suggest that secondary clustering of initially formed CD95L-CD95 complexes is of pivotal relevance. The well documented observation that oligomerization of soluble CD95L trimers and cross-linking of CD95-specific agonistic antibodies results in a much higher capability of these reagents to engage CD95 signaling (8, 49) could reflect such a special need of secondary clustering of CD95L-CD95 complexes in CD95 activation but could also simply reflect an avidity-mediated increase in appar-

FIGURE 7. **Activation of CD95-associated signaling pathways triggers redistribution of unliganded CD40-CD95 chimeras and unliganded endogenous CD95 molecules into the detergent-insoluble compartment.** *A* and *B*, the indicated HT1080 (*A*) and HaCaT (*B*) transfectants were stimulated for 2 h with 200 ng/ml Fc-FLAG-CD95L or 200 ng/ml Fc-FLAG-CD40L and subjected to lysis with Triton X-100 buffer and subsequent separation by sucrose density gradient centrifugation (*fraction 1*, insoluble membrane fraction with lipid rafts; *fraction 4*, soluble proteins). The intensity of the CD40-CD95 band of each fraction was quantified by LI-COR and normalized according to the total CD40-CD95 intensity of the corresponding gradient. Data shown are the average of three (*A*) and five (*B*) experiments. *C* and *D*, HaCaT-CD40-CD95 cells were transfected with control or caspase-8 specific siRNA. After 2 days, cells were stimulated for 2 h with 200 ng/ml Fc-FLAG-CD95L and were again analyzed by sucrose density gradient centrifugation and Western blotting for the distribution of the CD40-CD95 molecules. Western blot analysis of the sucrose density gradient fractions for CD40-CD95 distribution (*left panel*) and of total cell lysates for their caspase-8 content (*right panel*) are shown in *C* for one representative experiment. The averaged LI-COR quantification of CD40-CD95 distribution of five independent experiments is shown in *D*. *Tfr*, transferrin receptor. *E*, HT1080-CD40-CD95 and HaCaT-CD40-CD95 cells were incubated for 0.5 h with 25 ng/ml GpL-FLAG-CD95L to "label" a fraction of endogenous CD95 without activation of CD95-associated signaling pathways. Cells remained untreated or were then challenged with Fc-FLAG-CD40L for additional 2 h. Unbound ligands were removed by washing, and cells were lysed in Triton X-100 buffer and subjected to analysis by sucrose density gradient centrifugation. The distribution of the GpL-FLAG-CD95L was determined using a standard luciferase assay. Indicated is the mean ratio of relative light units of fraction 1 and fraction 4. *F*, a fraction of inactive endogenous CD95 of A498 cells was labeled by incubation with GpL-FLAG-CD95L (25 ng/ml) for 0.5 h. Remaining non-labeled CD95 molecules were then stimulated with Fc-FLAG-CD95L (200 ng/ml) for an additional 2 h. The distribution of GpL-FLAG-CD95L between the detergent soluble and insoluble compartment in stimulated and non-stimulated cells was then determined as in *E*. Shown is the average of three-five independent experiments (*E* and *F*). *G*, HT1080 cells were incubated for 30 min with GpL-FLAG-CD95L to mark inactive CD95 complexes and were then challenged for 4 h with RAPO cells, RAPO-CD95L cells, or RAPO cells supplemented with supernatant of RAPO-CD95L cells containing soluble CD95L (*RAPO*+SN_{CD95L}). Triton X-100 lysates were separated by sucrose density gradient centrifugation, and the fractions obtained were analyzed by Western blotting (*left panel*) and luciferase activity assay (*right panel*) for the presence of CD95 and GpL-FLAG-CD95L. Analysis of luciferase activity shown is derived from four independent experiments.

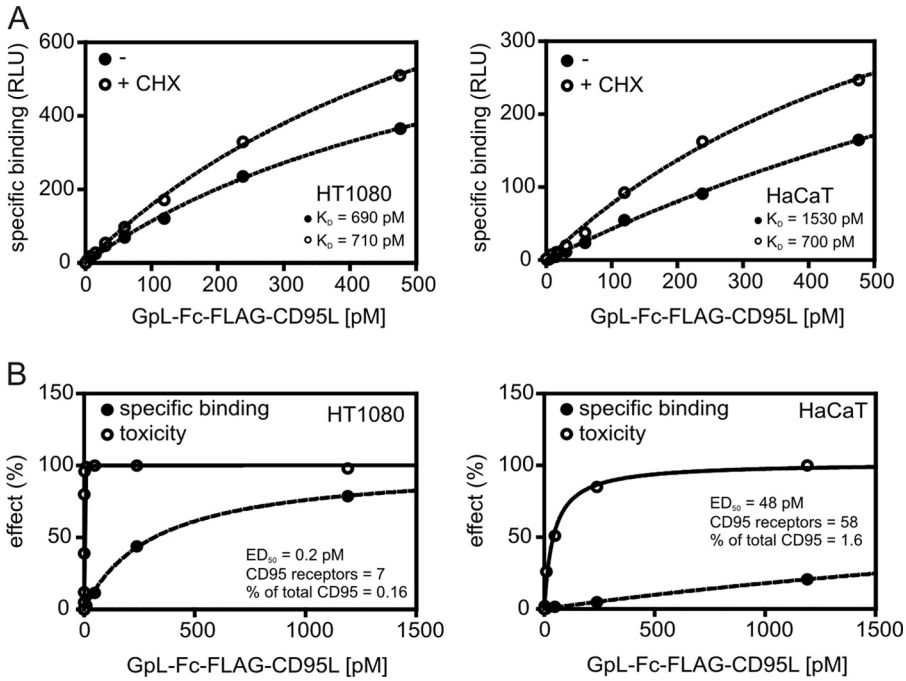

FIGURE 8. **A small fraction of CD95 is sufficient to trigger cell death.** *A*, the indicated cell lines (24-well plate) were treated with 2. 5 μg/ml CHX for 3 h or remained untreated and were then subjected to equilibrium binding studies at 37 °C with GpL-Fc-FLAG-CD95L as described under "Experimental Procedures." *RLU*, relative light units. *B*, cells were seeded in 96-well plates (2×10^4 cells per well) and were sensitized the next day for apoptosis induction by priming for 3 h with CHX. Cells were then treated with the indicated concentrations of GpL-Fc-FLAG-CD95L for 18 h, and viability was determined by crystal violet staining. In parallel, cells cultivated in 24-well plates were treated in the same fashion but were rescued from apoptosis by the addition of 20 μM caspase inhibitor zVAD-fmk and used for analysis of cell-specific binding of GpL-Fc-FLAG-CD95L. Ligand binding was normalized against the maximum binding calculated from the binding curve, and toxicity was normalized by help of a sample where cells have been treated with a killing mixture containing 80 μg/ml CHX and high doses of Fc-FLAG-CD95L. The average number of GpL-Fc-FLAG-CD95L-occupied CD95 trimers where cell death was induced in 50% of cells is indicated.

ent affinity and thus increased receptor occupancy by the oligomerized reagents.

Although it is evident from qualitative studies that soluble CD95L is generally able to interact with cellular CD95, this basic issue has not been addressed so far by rigorous correlation of ligand occupancy of CD95 and CD95 activation. This is not at least due to the difficulties in labeling of CD95L for cellular binding studies by conventional methods (*e.g.* iodination, biotinylation) without losing bioactivity and without yielding mixtures of molecules that differ in the degree of labeling and the sites modified. To overcome these limitations, we looked for a method to label CD95L by genetic engineering. This means we looked for a reporter protein domain that can be linked to soluble CD95L without affecting the molecule capability to interact with CD95. We evaluated various established reporter proteins/peptides including YFP and *M. longa* luciferase as well as SNAP (a mutant of O^6-alkylguanine-DNA alkyltransferase), but all the corresponding CD95L fusion proteins turned out to be aggregated and/or showed unacceptable low sensitivity (Fig. 3, *A* and *B*). However, it turned out that the secretable monomeric luciferase of *G. princeps* (GpL) is a perfect labeling domain for CD95L (and other TNF ligands). Genetic fusion of GpL to the N terminus of soluble CD95L or the Fc-CD95L fusion protein showed no major effect either on the specific activity of these molecules or, in case of trimeric CD95L, on the requirement for oligomerization to become highly active (Fig. 3, *E* and *F*). The GpL-CD95L fusion proteins further showed an excellent traceability allowing the detection of specific CD95L binding with the use of sub-pM concentrations and less than 10^6 cells per sample (Fig. 4).

With the help of the GpL-CD95L fusion proteins, it was possible to determine the signaling output of CD95 simulation (cell death, IL8) directly as a function of receptor occupancy. Although, as mentioned above, anti-FLAG oligomerized soluble GpL-FLAG-CD95L and hexameric GpL-Fc-FLAG-CD95L showed the known 2–3 orders of magnitude lower ED_{50} values for apoptotic and non-apoptotic CD95 signaling, the K_D values measured for these molecule species for CD95 binding were found to be close to those of the trimeric GpL-FLAG-CD95L variant (*e.g.* 1200 and 2600 to 2000 pM for HT1080; Fig. 4, *D* and *E*; Table 1). Although the oligomerized CD95L variants display a >100-fold higher specific activity than trimeric soluble CD95L molecules for apoptosis induction and IL8 up-regulation (Figs. 1 and 3), the latter triggers these responses too at high supraphysiological concentrations. It is currently not possible to decide whether this is due to percent/per mill traces of aggregates in samples of trimeric CD95L variants or if this reflects a weak intrinsic capacity of CD95 to cluster in response to binding of soluble CD95L trimers. In any case, however, it is clear from these data that the capacity of CD95 to engage apoptotic and proinflammatory signaling in response to soluble trimeric forms of CD95L is strongly enhanced by exogenously enforced dimerization/oligomerization of CD95L-CD95 complexes. This is in good accordance with the fact that both apoptosis induction and NFκB-mediated IL8 production by CD95 are FADD- and caspase-8-dependent and that the DDs of

FADD and CD95 form an oligomeric complex containing 10–12 DDs (20, 50). Noteworthy, there is growing evidence that soluble CD95L alone is sufficient to drive non-apoptotic responses (51–53). For example, it has been shown that soluble CD95L triggers activation of the PI3K/Akt pathway and cell migration by recruitment and stimulation of the Src family kinase cYes (51, 52). Especially, activation of this Akt-cYes occurred without FADD recruitment to CD95 (51, 52). Thus, it appears that soluble CD95L-induced Src/PI3K/Akt signaling and membrane CD95L-induced apoptosis and NFκB activation, both depending on FADD (5), involve fundamental different CD95-associated activation mechanisms. Although the studies cited have not addressed the consequences of oligomerization of soluble CD95L for signal strength, it appears possible that the activation of FADD-independent pathways by CD95 is already accomplished by trimeric CD95L-CD95 complexes. In fact, a differential requirement of ligand oligomerization for the activation of distinct signaling pathways stimulated by the same TNF receptor type was recently observed by us in the TWEAK-Fn14 system (54). On the other hand, soluble CD95L can be secondarily activated naturally by binding to the extracellular matrix or aggregation due to an oxidative microenvironment (14, 15), and it is thus not fully ruled out that such or related mechanisms play a role in the studies discussed above.

The observed K_D values for the interaction of CD95 with the various CD95L variants were rather high compared with the related ligand-receptor pair TNF-TNFR1 for which K_D values between 20–200 pM have been reported (55–58). The lower K_D value of the CD95L-CD95 interaction is mainly due to slower CD95L association, which takes 8–12 min to reach 50% of equilibrium binding at concentrations between 5 and 250 ng/ml (Fig. 4*G*). The comparatively slow association is in good accordance with the time course of signaling complex formation and IκBα degradation by CD95, which starts typically after 15–30 min post-addition of Fc-FLAG-CD95L (data not shown and Fig. 1*C*). Thus, the "delayed" time course of activation of CD95-associated pathways might mainly reflect the time required for initial binding of CD95L to CD95, whereas the subsequent steps leading to triggering of intracellular pathways are rather fast. CD95-induced apoptosis shows a threshold behavior with the concentrations of CD95L, thus the fraction/number of activated CD95 molecules, and $FLIP_{L/S}$ as the major determinants (59, 60). Accordingly, we observed in CHX-primed cells, under conditions where the concentrations of FLIP proteins are severely reduced (supplemental Fig. S1), that a very small number of occupied CD95 molecules is sufficient to trigger half-maximal killing (Fig. 8*B*).

Several studies have addressed the association of CD95 with the lipid raft-containing detergent-insoluble membrane compartment. There is typically low basal retention of CD95 in this compartment that is, however, increased in response to CD95 activation. Dependent on the cell type and the CD95-activating reagent used for stimulation (agonistic antibodies, aggregated soluble CD95L, membrane CD95L expressing cells) association with the lipid raft-containing membrane compartment is of varying relevance for apoptosis induction. Particularly, it has been found that a feed forward loop of caspase-8 activation contributes to activation-induced redistribution of CD95 into the insoluble membrane fraction (29). In accordance with the latter finding, we noted that soluble CD95L trimers that not or only poorly stimulate caspase-8 activation and apoptosis failed to increase lipid raft association of CD95 (Figs. 1*E* and 5). In contrast, when recombinant trimeric variants of soluble CD95L were converted into highly active CD95 agonists by oligomerization or cell surface immobilization, this comes along with enhanced stimulation of CD95 lipid raft association (Fig. 1). In accordance with the idea that oligomerization and cell surface immobilization of soluble CD95L variants convert these molecules in proteins with membrane CD95L-like activity, we further observed that membrane CD95L expressing cells, but not supernatants of these cells containing soluble CD95L molecules, also stimulated CD95 redistribution into lipid rafts (Fig. 2). Thus, the two naturally occurring forms of CD95L, soluble CD95L and membrane CD95L, not only differ in their capability to stimulate CD95-mediated apoptosis but also in their capability to trigger lipid raft association of CD95. The molecular functioning of the feed forward loop of caspase-8 activation in CD95 redistribution in the lipid raft compartment was quite unclear because it was not possible so far to measure and manipulate active and inactive CD95 species in parallel in a single experimental approach. We overcome this limitation here by the help of two novel approaches (i) by using for CD95 activation mixtures of highly active CD95L variants (Fc-FLAG-CD95L, membrane CD95L-expressing cells) and GpL-FLAG-CD95L whereby binding of the latter tags inactive CD95 species in the presence of activated CD95 molecules (Fig. 7, *F* and *G*) and (ii) by means of chimeric CD40-CD95 receptors allowing triggering of CD95-associated pathways in the presence of non-activated CD95 wild-type molecules (Fig. 7). With these novel tools we revealed (i) that signaling active CD95 species trigger the co-association of inactive CD95 molecules with the lipid raft compartment in a caspase-8-dependent fashion (Fig. 7, *C* and *D*) and (ii) that the capability of the CD95 cytoplasmic domain to recruit FADD is therefore required (Fig. 7, *A* and *B*). In view of the oligomeric structure of the complex of the DDs of CD95 and FADD and the fact that FADD-associated procaspase-8 forms homodimers or heterodimerizes with FADD-bound FLIP proteins, it is tempting to speculate that signaling active and inactive CD95 species are bridged by FADD and caspase-8. According to this very speculative idea, there is in unstimulated cells an equilibrium between very low levels of unstable CD95-FADD-caspase-8 complexes that have an intrinsic affinity to the lipid raft compartment and the corresponding "free" molecules. Binding of oligomerized soluble CD95L trimers might stabilize these complexes resulting in signaling and enhanced presence in the lipid raft compartment and constituting a condensation nucleus for the improved recruitment of additional CD95, FADD, and caspase-8 molecules. Previous reports showing that CD95L forms less stable complexes with CD95 variants that are unable to recruit FADD are in good accordance with the proposed model (18, 19). It would also be consistent with various reports showing

CD95L-independent CD95-mediated apoptosis in the situation of membrane stress (61–64).

Acknowledgments—We thank Renata R. Polakowska (Department of Dermatology, University of Rochester School of Medicine and Dentistry, Rochester, New York) for providing HaCaT-Bcl2 and the corresponding control cells. We are grateful to Martina Jossberger (Department of Dermatology, University Hospital Würzburg) for technical assistance with the caspase-8 siRNA experiments.

REFERENCES

1. Locksley, R. M., Killeen, N., and Lenardo, M. J. (2001) The TNF and TNF receptor superfamilies. Integrating mammalian biology. *Cell* **104,** 487–501
2. Sancho-Martinez, I., and Martin-Villalba, A. (2009) Tyrosine phosphorylation and CD95. A FAScinating switch. *Cell Cycle* **8,** 838–842
3. Wajant, H., Pfizenmaier, K., and Scheurich, P. (2003) Non-apoptotic Fas signaling. *Cytokine Growth Factor Rev.* **14,** 53–66
4. Holler, N., Zaru, R., Micheau, O., Thome, M., Attinger, A., Valitutti, S., Bodmer, J. L., Schneider, P., Seed, B., and Tschopp, J. (2000) Fas triggers an alternative, caspase-8-independent cell death pathway using the kinase RIP as effector molecule. *Nat. Immunol.* **1,** 489–495
5. Kreuz, S., Siegmund, D., Rumpf, J. J., Samel, D., Leverkus, M., Janssen, O., Häcker, G., Dittrich-Breiholz, O., Kracht, M., Scheurich, P., and Wajant, H. (2004) NFκB activation by Fas is mediated through FADD, caspase-8, and RIP and is inhibited by FLIP. *J. Cell Biol.* **166,** 369–380
6. Bodmer, J. L., Schneider, P., and Tschopp, J. (2002) The molecular architecture of the TNF superfamily. *Trends Biochem. Sci.* **27,** 19–26
7. Holler, N., Tardivel, A., Kovacsovics-Bankowski, M., Hertig, S., Gaide, O., Martinon, F., Tinel, A., Deperthes, D., Calderara, S., Schulthess, T., Engel, J., Schneider, P., and Tschopp, J. (2003) Two adjacent trimeric Fas ligands are required for Fas signaling and formation of a death-inducing signaling complex. *Mol. Cell. Biol.* **23,** 1428–1440
8. Schneider, P., Holler, N., Bodmer, J. L., Hahne, M., Frei, K., Fontana, A., and Tschopp, J. (1998) Conversion of membrane-bound Fas(CD95) ligand to its soluble form is associated with down-regulation of its proapoptotic activity and loss of liver toxicity. *J. Exp. Med.* **187,** 1205–1213
9. Suda, T., Hashimoto, H., Tanaka, M., Ochi, T., and Nagata, S. (1997) Membrane Fas ligand kills human peripheral blood T lymphocytes, and soluble Fas ligand blocks the killing. *J. Exp. Med.* **186,** 2045–2050
10. Tanaka, M., Itai, T., Adachi, M., and Nagata, S. (1998) Down-regulation of Fas ligand by shedding. *Nat. Med.* **4,** 31–36
11. Bremer, E., ten Cate, B., Samplonius, D. F., de Leij, L. F., and Helfrich, W. (2006) CD7-restricted activation of Fas-mediated apoptosis. A novel therapeutic approach for acute T-cell leukemia. *Blood* **107,** 2863–2870
12. Bremer, E., ten Cate, B., Samplonius, D. F., Mueller, N., Wajant, H., Stel, A. J., Chamuleau, M., van de Loosdrecht, A. A., Stieglmaier, J., Fey, G. H., and Helfrich, W. (2008) Superior activity of fusion protein scFvRit:sFasL over cotreatment with rituximab and Fas agonists. *Cancer Res.* **68,** 597–604
13. Samel, D., Muller, D., Gerspach, J., Assohou-Luty, C., Sass, G., Tiegs, G., Pfizenmaier, K., and Wajant, H. (2003) Generation of a FasL-based proapoptotic fusion protein devoid of systemic toxicity due to cell-surface antigen-restricted activation. *J. Biol. Chem.* **278,** 32077–32082
14. Herrero, R., Kajikawa, O., Matute-Bello, G., Wang, Y., Hagimoto, N., Mongovin, S., Wong, V., Park, D. R., Brot, N., Heinecke, J. W., Rosen, H., Goodman, R. B., Fu, X., and Martin, T. R. (2011) The biological activity of FasL in human and mouse lungs is determined by the structure of its stalk region. *J. Clin. Invest.* **121,** 1174–1190
15. Aoki, K., Kurooka, M., Chen, J. J., Petryniak, J., Nabel, E. G., and Nabel, G. J. (2001) Extracellular matrix interacts with soluble CD95L. Retention and enhancement of cytotoxicity. *Nat. Immunol.* **2,** 333–337
16. Guicciardi, M. E., and Gores, G. J. (2009) Life and death by death receptors. *FASEB J.* **23,** 1625–1637
17. Schütze, S., Tchikov, V., and Schneider-Brachert, W. (2008) Regulation of TNFR1 and CD95 signaling by receptor compartmentalization. *Nat. Rev. Mol. Cell Biol.* **9,** 655–662
18. Henkler, F., Behrle, E., Dennehy, K. M., Wicovsky, A., Peters, N., Warnke, C., Pfizenmaier, K., and Wajant, H. (2005) The extracellular domains of FasL and Fas are sufficient for the formation of supramolecular FasL-Fas clusters of high stability. *J. Cell Biol.* **168,** 1087–1098
19. Siegel, R. M., Muppidi, J. R., Sarker, M., Lobito, A., Jen, M., Martin, D., Straus, S. E., and Lenardo, M. J. (2004) SPOTS. Signaling protein oligomeric transduction structures are early mediators of death receptor-induced apoptosis at the plasma membrane. *J. Cell Biol.* **167,** 735–744
20. Wang, L., Yang, J. K., Kabaleeswaran, V., Rice, A. J., Cruz, A. C., Park, A. Y., Yin, Q., Damko, E., Jang, S. B., Raunser, S., Robinson, C. V., Siegel, R. M., Walz, T., and Wu, H. (2010) The Fas-FADD death domain complex structure reveals the basis of DISC assembly and disease mutations. *Nat. Struct. Mol. Biol.* **17,** 1324–1329
21. Eramo, A., Sargiacomo, M., Ricci-Vitiani, L., Todaro, M., Stassi, G., Messina, C. G., Parolini, I., Lotti, F., Sette, G., Peschle, C., and De Maria, R. (2004) CD95 death-inducing signaling complex formation and internalization occur in lipid rafts of type I and type II cells. *Eur. J. Immunol.* **34,** 1930–1940
22. Gajate, C., and Mollinedo, F. (2001) The antitumor ether lipid ET-18-OCH(3) induces apoptosis through translocation and capping of Fas/CD95 into membrane rafts in human leukemic cells. *Blood* **98,** 3860–3863
23. Grassmé, H., Cremesti, A., Kolesnick, R., and Gulbins, E. (2003) Ceramide-mediated clustering is required for CD95-DISC formation. *Oncogene* **22,** 5457–5470
24. Grassme, H., Jekle, A., Riehle, A., Schwarz, H., Berger, J., Sandhoff, K., Kolesnick, R., and Gulbins, E. (2001) CD95 signaling via ceramide-rich membrane rafts. *J. Biol. Chem.* **276,** 20589–20596
25. Grassmé, H., Schwarz, H., and Gulbins, E. (2001) Molecular mechanisms of ceramide-mediated CD95 clustering. *Biochem. Biophys. Res. Commun.* **284,** 1016–1030
26. Chakrabandhu, K., Hérincs, Z., Huault, S., Dost, B., Peng, L., Conchonaud, F., Marguet, D., He, H. T., and Hueber, A. O. (2007) Palmitoylation is required for efficient Fas cell death signaling. *EMBO J.* **26,** 209–220
27. Feig, C., Tchikov, V., Schütze, S., and Peter, M. E. (2007) Palmitoylation of CD95 facilitates formation of SDS-stable receptor aggregates that initiate apoptosis signaling. *EMBO J.* **26,** 221–231
28. Rossin, A., Kral, R., Lounnas, N., Chakrabandhu, K., Mailfert, S., Marguet, D., and Hueber, A. O. (2010) Identification of a lysine-rich region of Fas as a raft nanodomain targeting signal necessary for Fas-mediated cell death. *Exp. Cell Res.* **316,** 1513–1522
29. Algeciras-Schimnich, A., Shen, L., Barnhart, B. C., Murmann, A. E., Burkhardt, J. K., and Peter, M. E. (2002) Molecular ordering of the initial signaling events of CD95. *Mol. Cell. Biol.* **22,** 207–220
30. Lee, K. H., Feig, C., Tchikov, V., Schickel, R., Hallas, C., Schütze, S., Peter, M. E., and Chan, A. C. (2006) The role of receptor internalization in CD95 signaling. *EMBO J.* **25,** 1009–1023
31. Parlato, S., Giammarioli, A. M., Logozzi, M., Lozupone, F., Matarrese, P., Luciani, F., Falchi, M., Malorni, W., and Fais, S. (2000) CD95 (APO-1/Fas) linkage to the actin cytoskeleton through ezrin in human T lymphocytes. A novel regulatory mechanism of the CD95 apoptotic pathway. *EMBO J.* **19,** 5123–5134
32. Janssen, O., Lengl-Janssen, B., Oberg, H. H., Robertson, M. J., and Kabelitz, D. (1996) Induction of cell death via Fas (CD95, Apo-1) may be associated with, but is not dependent on Fas-induced tyrosine phosphorylation. *Immunol Lett.* **49,** 63–69
33. Haake, A. R., and Polakowska, R. R. (1995) UV-induced apoptosis in skin equivalents. Inhibition by phorbol ester and Bcl-2 overexpression. *Cell Death Differ.* **2,** 183–193
34. Siegmund, D., Wicovsky, A., Schmitz, I., Schulze-Osthoff, K., Kreuz, S., Leverkus, M., Dittrich-Breiholz, O., Kracht, M., and Wajant, H. (2005) Death receptor-induced signaling pathways are differentially regulated by γ interferon upstream of caspase 8 processing. *Mol. Cell. Biol.* **25,** 6363–6379
35. Wajant, H., Gerspach, J., and Pfizenmaier, K. (2011) *Cancer Lett.*, in press
36. Tannous, B. A., Kim, D. E., Fernandez, J. L., Weissleder, R., and Breakefield, X. O. (2005) Codon-optimized Gaussia luciferase cDNA for mammalian gene expression in culture and *in vivo*. *Mol. Ther.* **11,** 435–443

37. Berg, D., Lehne, M., Müller, N., Siegmund, D., Münkel, S., Sebald, W., Pfizenmaier, K., and Wajant, H. (2007) Enforced covalent trimerization increases the activity of the TNF ligand family members TRAIL and CD95L. *Cell Death Differ.* **14,** 2021–2034
38. Wyzgol, A., Müller, N., Fick, A., Munkel, S., Grigoleit, G. U., Pfizenmaier, K., and Wajant, H. (2009) Trimer stabilization, oligomerization, and antibody-mediated cell surface immobilization improve the activity of soluble trimers of CD27L, CD40L, 41BBL, and glucocorticoid-induced TNF receptor ligand. *J. Immunol.* **183,** 1851–1861
39. Barnhart, B. C., Alappat, E. C., and Peter, M. E. (2003) The CD95 type I/type II model. *Semin. Immunol.* **15,** 185–193
40. Hao, Z., and Mak, T. W. (2010) Type I and type II pathways of Fas-mediated apoptosis are differentially controlled by XIAP. *J Mol. Cell. Biol.* **2,** 63–64
41. Martin, D. A., Zheng, L., Siegel, R. M., Huang, B., Fisher, G. H., Wang, J., Jackson, C. E., Puck, J. M., Dale, J., Straus, S. E., Peter, M. E., Krammer, P. H., Fesik, S., and Lenardo, M. J. (1999) Defective CD95/APO-1/Fas signal complex formation in the human autoimmune lymphoproliferative syndrome, type Ia. *Proc. Natl. Acad. Sci. U.S.A.* **96,** 4552–4557
42. Bossen, C., Ingold, K., Tardivel, A., Bodmer, J. L., Gaide, O., Hertig, S., Ambrose, C., Tschopp, J., and Schneider, P. (2006) Interactions of tumor necrosis factor (TNF) and TNF receptor family members in the mouse and human. *J. Biol. Chem.* **281,** 13964–13971
43. Fulda, S., Meyer, E., and Debatin, K. M. (2000) Metabolic inhibitors sensitize for CD95 (APO-1/Fas)-induced apoptosis by down-regulating Fas-associated death domain-like interleukin 1-converting enzyme inhibitory protein expression. *Cancer Res.* **60,** 3947–3956
44. Imanishi, T., Hano, T., Nishio, I., Liles, W. C., Schwartz, S. M., and Han, D. K. (2000) Transition of apoptotic-resistant vascular smooth muscle cells to troptotic sensitive state is correlated with down-regulation of c-FLIP. *J. Vasc. Res.* **37,** 523–531
45. Kreuz, S., Siegmund, D., Scheurich, P., and Wajant, H. (2001) NF-κB inducers up-regulate cFLIP, a cycloheximide-sensitive inhibitor of death receptor signaling. *Mol. Cell. Biol.* **21,** 3964–3973
46. Siegmund, D., Hadwiger, P., Pfizenmaier, K., Vornlocher, H. P., and Wajant, H. (2002) Selective inhibition of FLICE-like inhibitory protein expression with small interfering RNA oligonucleotides is sufficient to sensitize tumor cells for TRAIL-induced apoptosis. *Mol. Med.* **8,** 725–732
47. Papoff, G., Hausler, P., Eramo, A., Pagano, M. G., Di Leve, G., Signore, A., and Ruberti, G. (1999) Identification and characterization of a ligand-independent oligomerization domain in the extracellular region of the CD95 death receptor. *J. Biol. Chem.* **274,** 38241–38250
48. Siegel, R. M., Frederiksen, J. K., Zacharias, D. A., Chan, F. K., Johnson, M., Lynch, D., Tsien, R. Y., and Lenardo, M. J. (2000) Fas preassociation required for apoptosis signaling and dominant inhibition by pathogenic mutations. *Science* **288,** 2354–2357
49. Kischkel, F. C., Hellbardt, S., Behrmann, I., Germer, M., Pawlita, M., Krammer, P. H., and Peter, M. E. (1995) Cytotoxicity-dependent APO-1 (Fas/CD95)-associated proteins form a death-inducing signaling complex (DISC) with the receptor. *EMBO J.* **14,** 5579–5588
50. Esposito, D., Sankar, A., Morgner, N., Robinson, C. V., Rittinger, K., and Driscoll, P. C. (2010) Solution NMR investigation of the CD95/FADD homotypic death domain complex suggests a lack of engagement of the CD95 C terminus. *Structure* **18,** 1378–1390
51. Kleber, S., Sancho-Martinez, I., Wiestler, B., Beisel, A., Gieffers, C., Hill, O., Thiemann, M., Mueller, W., Sykora, J., Kuhn, A., Schreglmann, N., Letellier, E., Zuliani, C., Klussmann, S., Teodorczyk, M., Gröne, H. J., Ganten, T. M., Sültmann, H., Tüttenberg, J., von Deimling, A., Regnier-Vigouroux, A., Herold-Mende, C., and Martin-Villalba, A. (2008) Yes and PI3K bind CD95 to signal invasion of glioblastoma. *Cancer Cell* **13,** 235–248
52. Tauzin, S., Chaigne-Delalande, B., Selva, E., Khadra, N., Daburon, S., Contin-Bordes, C., Blanco, P., Le Seyec, J., Ducret, T., Counillon, L., Moreau, J. F., Hofman, P., Vacher, P., and Legembre, P. (2011) The naturally processed CD95L elicits a c-yes/calcium/PI3K-driven cell migration pathway. *PLoS Biol.* **9,** e1001090
53. O' Reilly, L.A., Tai, L., Lee, L., Kruse, E. A., Grabow, S., Fairlie, W. D., Haynes, N. M., Tarlinton, D. M., Zhang, J. G., Belz, G. T., Smyth, M. J., Bouillet, P., Robb, L., and Strasser, A. (2009) Membrane-bound Fas ligand only is essential for Fas-induced apoptosis. *Nature* **461,** 659–663
54. Roos, C., Wicovsky, A., Müller, N., Salzmann, S., Rosenthal, T., Kalthoff, H., Trauzold, A., Seher, A., Henkler, F., Kneitz, C., and Wajant, H. (2010) Soluble and transmembrane TNF-like weak inducer of apoptosis differentially activates the classical and noncanonical NF-κ B pathway. *J. Immunol.* **185,** 1593–1605
55. Aggarwal, B. B., Eessalu, T. E., and Hass, P. E. (1985) Characterization of receptors for human tumornecrosis factor and their regulation by γ-interferon. *Nature* **318,** 665–667
56. Baglioni, C., McCandless, S., Tavernier, J., and Fiers, W. (1985) Binding of human tumor necrosis factor to high affinity receptors on HeLa and lymphoblastoid cells sensitive to growth inhibition. *J. Biol. Chem.* **260,** 13395–13397
57. Grell, M., Wajant, H., Zimmermann, G., and Scheurich, P. (1998) The type 1 receptor (CD120a) is the high affinity receptor for soluble tumor necrosis factor. *Proc. Natl. Acad. Sci. U.S.A.* **95,** 570–575
58. Smith, R. A., and Baglioni, C. (1987) The active form of tumor necrosis factor is a trimer. *J. Biol. Chem.* **262,** 6951–6954
59. Bentele, M., Lavrik, I., Ulrich, M., Stösser, S., Heermann, D. W., Kalthoff, H., Krammer, P. H., and Eils, R. (2004) Mathematical modeling reveals threshold mechanism in CD95-induced apoptosis. *J. Cell Biol.* **166,** 839–851
60. Lavrik, I. N., Golks, A., Riess, D., Bentele, M., Eils, R., and Krammer, P. H. (2007) Analysis of CD95 threshold signaling. Triggering of CD95 (FAS/APO-1) at low concentrations primarily results in survival signaling. *J. Biol. Chem.* **282,** 13664–13671
61. Faubion, W. A., Guicciardi, M. E., Miyoshi, H., Bronk, S. F., Roberts, P. J., Svingen, P. A., Kaufmann, S. H., and Gores, G. J. (1999) Toxic bile salts induce rodent hepatocyte apoptosis via direct activation of Fas. *J. Clin. Invest.* **103,** 137–145
62. Fumarola, C., Zerbini, A., and Guidotti, G. G. (2001) Glutamine deprivation-mediated cell shrinkage induces ligand-independent CD95 receptor signaling and apoptosis. *Cell Death Differ.* **8,** 1004–1013
63. Gajate, C., Fonteriz, R. I., Cabaner, C., Alvarez-Noves, G., Alvarez-Rodriguez, Y., Modolell, M., and Mollinedo, F. (2000) Intracellular triggering of Fas, independently of FasL, as a new mechanism of antitumor ether lipid-induced apoptosis. *Int. J. Cancer* **85,** 674–682
64. Micheau, O., Solary, E., Hammann, A., and Dimanche-Boitrel, M. T. (1999) Fas ligand-independent, FADD-mediated activation of the Fas death pathway by anticancer drugs. *J. Biol. Chem.* **274,** 7987–7992